IJEGEO
International Journal of Environment and Geoinformatics 10(4):117-145 (2023)

Research Article

Application of Geoinformatics in Civil Engineering Design and Construction: A Case Study of Ile Oluji, SW Nigeria

Olumuyiwa Olusola Falowo

Department of Applied Geology, Federal University of Technology Akure, Ondo State, Nigeria

* E-mail: oofalowo@futa.edu.ng

Received:08.03.2023
Accepted: 16.12.2023

How to cite: Falowo, O. (2023). Application of Geoinformatics in Civil Engineering Design and Construction: A Case Study of Ile Oluji, Southwestern Nigeria, *International Journal of Environment and Geoinformatics (IJEGEO)*, 10(4): 117-145. doi. 10.30897/ijegeo.1262020

Abstract

Subsoil engineering site condition and modeling of engineering parameters had been carried out in Ile Oluji, Ondo State, Southwestern Nigeria, using geotechnical investigation, geophysical method, borehole logging, groundwater level measurement, and laboratory studies. Findings revealed that the soils are clayey of low-high plasticity/compressibility, with AASHTO classification of A-7-6. Based on average values of cohesion (48.4 KN/m^2), angle of friction (17.4°), unconfined compressive strength (186.8 KN/m^2), coefficient of permeability (2.13E-06 cm/s), activity (0.48), soaked CBR (7 %), MDD/OMC (1980 kg/m^3/14.8 %), plasticity index (20.2 %), group index (6 %), compression index (0.0443), coefficient of volume compressibility (0.2041 m2/KN), depth to basement rock (22.2 m), static water levels 5.5 m (in well) and 21.8 m (in borehole), the soil is unsuitable for highway subgrade, subbase, and base courses. Thus, if it is expedient to use it as subgrade soil, the minimum recommended thickness is 241 – 513 mm (avg. 395 mm). The average allowable bearing capacity of the soil for square and round foundations are 268.4 KN/m^2 and 267.95 KN/m^2 respectively, with average total settlement of 18.3 mm for structural pressure of 100 KN/m^2. For embankment, the suitability index (1.21) of the soil suggests a fair/expanding not collapsible construction material. The rock units in the area have high compressive/shear strength, modulus of elasticity, high crushing strength, low deformability; and presumable bearing capacity of 8, 000 – 10, 000 KPa when fresh, and 5000 – 7000 KPa when partly or slightly weathered. Consequently, they are valuable as foundation constructions, aggregate in pavement, building stone, and armourstones. The correlation coefficient of the parameters are: MDD/PI vs. CBR (0.0043), LL vs. coefficient of consolidation (0.0608), PI vs. undrained shear strength/effective overburden (0.2706), PI vs. angle of shearing (0.0117), dry density vs. angle of shearing (0.0058), suitability index vs. CBRs (0.3644), clay contents vs. PI (0.1355).

Keywords: Embankment, Pavement, Geoinformatics, Geotechnics

Introduction

Geoinformatics is the branch of science that employs scientific procedures or techniques to solve problems in geography, cartography, geosciences, and related fields of science and engineering (Alaminiokuma and Chaanda, 2020; Eebo et al., 2022; Bawallah et al., 2021; Kumari and Somvanshi, 2017; Sabins, 1996). It is concerned with the acquisition of geo-data in order to improve knowledge and interpretation of human interaction with the earth's surface. It encompasses a wide range of technologies, approaches, processes, and strategies. Geoinformation can combine various kinds of datasets from geographic information systems (GIS), remote sensing, and non-remote sensing to produce maps or other forms of report (Kumari and Somvanshi, 2017). Geoinformatics is a powerful technology that can support fundamental scientific research as well as address a variety of complex social and environmental issues. It enables civil engineers to easily organize, share, reuse, and analyze data in civil engineering construction, allowing them to better control time and resources (Kennie and Matthews, 1985; Lillesland et al., 2003). In summary, it aids in data management, visualization, and integration; infrastructure management; critical infrastructure protection of utilities, bridges, and so on; landfill site assessment; urban development and town planning (sanitation, power, waste supply, housing, environmental pollution, and effluent disposal); engineering site analysis; watershed management; transportation planning; construction management at a lower cost (Kumari and Somvanshi, 2017; Sabins, 1996). As a result, the importance of geoinformatics in site analysis (preconstruction data gathering and analysis) cannot be overstated. As a result, preconstruction site research is required for the construction of civil engineering projects in order to prevent failure due to capacity issues, settling, structure placement on fissures and joints systems, fracture, or underground stream channel. This reduces the degree of uncertainty of subsurface conditions, which can lead to unexpected or unbudgeted building structural changes (Kamtchueng et al., 2015; Coker, 2015; Olayanju et al., 2017; Roy, 2017; Ojo et al., 2015).

The features of the earth formation on which civil engineering infrastructure is built necessitated a well-planned subsurface study (Alabi et al., 2017; Faseki et al., 2016). This is prerequisite to safe economic design of foundation components of a structure (Osinowo and Falufosi, 2018; Oyedele et al., 2014). This will aid in the identification of unsuitable sites, such as those over deep coal mines, expansive shales or pyritic formations, highly compressible or highly expansive clays, landfill sites, and unusual subterranean water problems that may cause expensive foundation and building issues. Problems related to construction can also be catered for and recognized, such as a large volume of water infiltration into the excavation, which necessitates the need for a dewatering program, rock excavation, blasting of rock as it affects nearby structures, or general environmental conditions such as water supply (Tomlinson, 2001; Ward et al., 1968; Carter and Symons, 1989; Hawkins, 1986). Criteria must be specifically explored in subsoil investigation foundation design to determine what form of foundation is appropriate for locations. In order to determine the size, structure, and following specifics of the foundation, the bearing capacity or permissible bearing capacity must be established; particularly for shallow foundations (ordinary spread or isolated footings, combined footings or mats). Piles and caissons are examples of profound supports. For the construction of such components, knowledge on friction factors (for friction piles) and end-bearing values for piles and caissons derived from end (tip) support media is required (Craig, 1996).

The consolidation of the underlying clay layers causes the settlement of a building built on soil. Under excessive effective pressure, the overall compression of a clay strata is the aggregate of immediate, primary, and secondary compressions (Das, 2015). If the structure settles uniformly into the earth, there will be no negative impacts on the building as a whole. The only impact it may have is on utility lines, such as water and sewage sewer connections, telephone and electric wires, and so on, which may break if the settling is significant. This type of uniform settling is only feasible if the subsoil is homogeneous and the weight is uniform (Terzaghi, et al., 1996). Most of the time, the differential settlement between structural sections does not surpass 75% of the usual absolute settlement. The foundation settling must be approximated with extreme caution. Buildings, bridges, skyscrapers, power plants, and other high-cost constructions (such as fills and earth dams) have a wider margin of error.

Groundwater can influence the type of construction methodology that should be adopted to allow construction to proceed, knowing the depth of groundwater through groundwater assessment is good to know at the design stage and well before project/construction begins (Bell, 2007, 2004; Arora, 2008). Consequently, Geophysics and geotechnics through insitu and/or laboratory test are powerful tools used complimentarily in engineering site investigation (Coker, 2015; Olayanju et al., 2017; Alabi et al., 2017; Adewuyi and Philips, 2018; Adejumo et al., 2015). Geophysics can aid in the detection of anomalous regions linked with important subsurface characteristics. The discovery of anomalous zones can pave the way for experimental pits, ditches, and other types of boring for further study. As a result, electrical resistivity is a very efficient and environmentally favorable method of assessing engineering sites (Osinowo and Falufosi, 2018). The primary goals of this research are to gain a thorough knowledge of the technical and geological characteristics of soil and rock layers, as well as groundwater conditions in Ile Oluji, Nigeria; with research methods included in-situ and laboratory testing, assessment of subsoil features, bearing capacity evaluation, and obtaining significant soil's parameters correlation and dataset modeling.

Study Area

Ile Oluji is the study region, which is situated between 704800 m and 708800 m East and 793350 m and 809900 m North (Figure 1). It is bounded by the local governments of Ipetu-Ijesa, Ondo East/West, Ifetedo, Okeigbo, and Ifedore. Otasun Hills, Ikeji Hills, Okurughu, Oni River, and Awo River distinguish the region. The community is the administrative center of the Ile-Oluji/Okeigbo Local Council. Ile Oluji is an agravian village that is one of Nigeria's biggest producers and importers of cocoa. Farmers in the village primarily grow cassava, yam, corn, and oil palm. Cocoa Products Ile Oluji Limited is the town's main industrial firm. The major manufacturing company in the town is Cocoa Products Ile Oluji Limited. The Federal Polytechnic, Ile Oluji is a major tertiary institution in the town, while Gboluji Grammar school is the major high school in the area, and this school happens to be one of the oldest secondary school in Nigeria.

Physiography and Geology

The area is within the tropical rain forest with distinct wet and dry seasons. The annual rainfall varies between 1400 mm and 1800 mm. The mean temperature is 27°C and varies from 24.5°C in July to 29.5°C in February (Federal Meteorological Survey, 1982; Iloeje, 1981). The study area is underlain by Precambrian basement rocks (Figure 2) of impervious quality. The local geological rock units observed from outcrops showed the presence of granites, quartzite and migmatite-gneiss. Quartzite (ridges) and granite gneiss (Figure 2), but granite are the most widespread, while granite gneiss occurs as intrusive, low-lying outcrops. Field observation shows the presence of joints, fractures or faults within the bedrock. As a result, there is a greater likelihood of these characteristics at greater depth, as this is one of the peculiarities of the basement complex (i.e. fault, incipient joints, and fracture systems) that are a result of tectonic/orogenic processes that occur constantly. The fractured zone and weathered layer are the primary aquiferous units in a normal subterranean environment. Because it is frequently difficult to discern productive aquifers in the basement and describe their geometry, precise knowledge of the hydrogeological characteristics of the aquifer units and their vulnerability to environmental pollution is critical.

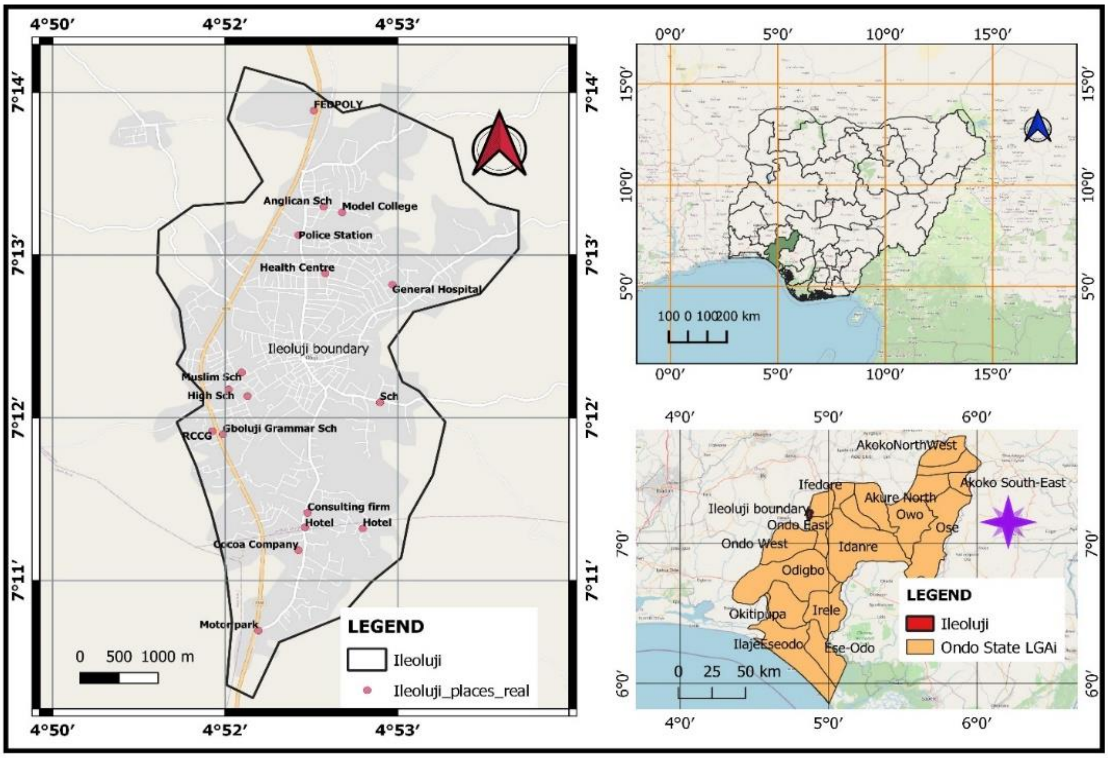

Fig. 1. Location map of Ile-oluji on Nigeria, and Ondo State maps

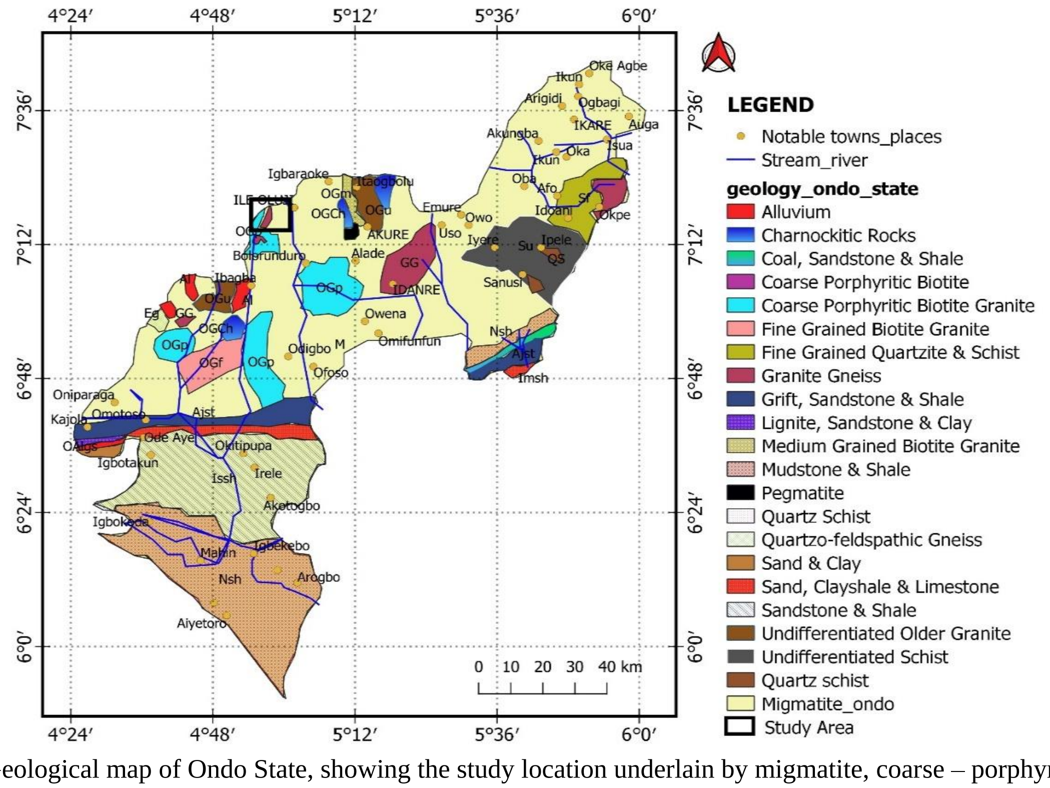

Fig. 2. Geological map of Ondo State, showing the study location underlain by migmatite, coarse – porphyritic Biotite Granite, and undifferentiated Older Granite (modified after NGSA, 1984, 2006)

Material and Methods

The character and scope of the site investigation are determined by the intended structure's utilization. As a result, the research study put into mind, conventional structures such as roads and buildings, earthwork and slope with different weight specifications. This is done in order to provide accurate baseline information or data to assist in the selection and planning of appropriate foundation/excavation. As a result, the technique used for this procedure included reconnaissance studies and thorough soil investigation. This was accomplished through extensive computer research and an examination of geotechnical and foundation literature. Before thorough planning could begin, the reconnaissance study

included an early feasibility study of the region. This aids in getting rough/sketchy knowledge or soil type.
During this research, a rough soil profile was created, and representative soil samples of the main soil strata were gathered, as well as the area's groundwater condition. This effort was thought to aid in deciding on a future exploration program. Furthermore, the terrain, drainage, and surficial soil features were evaluated, and the geological map and soil map were closely examined to support or validate/update the extant maps.

Figure 3 depicts the data collection map. The trial trenches are a simplistic and dependable technique of inquiry that allows for the collection of typical samples and the examination of geologic layers. For this research, 20 trial pits were excavated to a depth of 1 - 3 m using a hand-digger. The excavated sediment was put approximately 1.0 m away from the pits' edges. During the drill, no groundwater table was noted. The pit samples were taken from its sides/bottom (for disturbed samples), while tube samples were obtained below the pit's bottom (for undisturbed). The disturbed samples were gathered for the measurement of shear strength metrics and the consolidation test. The pits were immediately inspected and samples were gathered, they were sand filled after use. The use of trial pits allows the in-situ soil to be visibly inspected, allowing the boundaries between layers and the character of any macro-fabric to be precisely determined. For all fieldwork assessments, the GPS was used to record the positions of all sampling sites. The GPS is cost effective and time saving to traditional use of theodolites and levels. The geotechnical parameters were analyzed using America Standard for Testing and Material (ASTM, 2006) and British Standard (BS 1377, 1990) procedures, with the following tests: natural moisture content (D2216), grain size distribution (D422; D1140), specific gravity (D854; D5550), consistency limit and linear shrinkage (D4318), density (BS 1377), triaxial (D4767; D2850), unconfined compressive strength (D2166), permeability (D2434), compaction (D1557; D698), California Bearing Ratio, one dimensional consolidation (D4186; D4546). The in-situ CPT test was done following ASTM-D3441-94 procedures.

The CPT equipment utilized the Dutch cone penetrometer with an anvil, driving rod, and other accessories in nine locations. The machine nominal capacity was 10-tonnes and was operated by using hydraulically operated driving mechanism. The cone tip angle of the penetrometer used was 60° and rods of 100 cm long. In order to obtain the cone resistance value, the cone was pushed vertically at a rate of 2cm/s a depth of 0.25 m each time (Cetin and Ozan, 2009). Penetration resistance (q_c), sleeve friction (f_s) and the depth of penetration were recorded at each station and processed into plots. All the test reached refusal before the anchors pulled out of the subsurface. The layer sequences were interpreted using the Robertson Chart (Robertson, 1990), while cone resistance contrast between the various layers, inflection points of the penetrometer curves were interpreted as the interface between the different lithologies (Mayne, 2007; Robertson, 1990). Both qualitative and quantitative interpretation of the CPT readings in this study followed the guidelines of ASTM D5778. The CPT data was normalized to standard overburden pressure (q_{cn}) of 100 KN/m^2 (Moss et al., 2006). Hence from the result of the CPT, unconfined compressive strength (equation 1), ultimate bearing capacity was derived (equations 2 and 3), ultimate capacity (Q_{ult}) and elastic modulus for strip and square using equations 4, 5, and 6 respectively, SPT - N_{cor} (equations 7) and Modulus number (equation 8).

$$C_u = \frac{q_{cn}}{N_k} \quad \text{(Eq.1)}$$

where C_u is unconfined compressive strength, N_k is equal to 17 to 18 for normally consolidated clays or 20 for over consolidated clay. The bearing capacity using normalized cone resistance values was determined for D/B ≤ 1.5 (in kg/cm^2):

$$Strip: Q_{ult} = 2 + 0.28q_c \quad \text{(Eq.2)}$$

$$Square: Q_{ult} = 5 + 0.34q_c \quad \text{(Eq.3)}$$

$$Q_{ult} = \frac{Q_{cn}}{40}\ in\ kg/cm^2 \quad \text{(Eq.4)}$$

$$E_{strip} = 3.5 \times Q_{ult} \quad \text{(Eq.5)}$$

$$E_{square} = 2.5 \times Q_{ult} \quad \text{(Eq.6)}$$

$$N_{Cor} = \frac{Q_c}{4} \quad \text{(Eq.7)}$$

$$Modulus\ Number = 22.4 \times CBR^{0.5} \quad \text{(Eq.8)}$$

From the analysis, the followings were derived: settlement (both elastic and consolidation), activity (equation 9), Group Index (GI), AASHTO and USCS classifications, suitability index (equation 10), bearing pressure models were developed from CPT results using Hatanaka and Uchida (1996), Meyerhoff (1956), and Schmertmann (1975) equations; with corresponding stresses (mean, +ve, and –ve stresses) using Burland and Burbidge (1984) model.

Correlations were made between parameters: MDD/PI vs. CBR, LL vs. coefficient of consolidation, PI vs. undrained shear strength/effective overburden, PI vs. angle of shearing, dry density vs. angle of shearing, suitability index vs. CBR, clay contents vs. PI. Mineralogy and micro fabric of the clay structure are studied using X-ray diffraction, differential thermal analysis and scanning electron microscope. In this study, the geochemical analysis was done using X-ray diffraction.

$$A = \frac{PI}{\%\,finer\ than\ 2.0\ mm} \quad \text{(Eq. 9)}$$

$$S_i = \frac{\%\,finer\ than\ 2.0\ mm}{LL\log(PI)} \quad \text{(Eq. 10)}$$

The acquisition of VES data was in line with Falowo and Dahunsi (2020) and Falowo and Olabisi (2020) using Schlumberger array with maximum current – current spread of 130 m, and potential – potential distance of 5m. A total of fifty VES was acquired. The quantitative interpretation of the VES curves involved partial curve matching and computer iteration technique. This technique assumes that the earth is made up of horizontal layers with differing resistivity. Any significant deviation (in dip angle greater than 10%) from this planar assumption in the stratigraphy will slightly distort the VES curve and introduce error in the VES interpretation results. Other sources of error are lateral inhomogeneity, suppression and equivalence. All these were taken care of during data analysis and interpretation. The depth sounding interpretation are presented as geoelectric section, which showed horizontal to near horizontal stratification of the subsurface geologic layers.

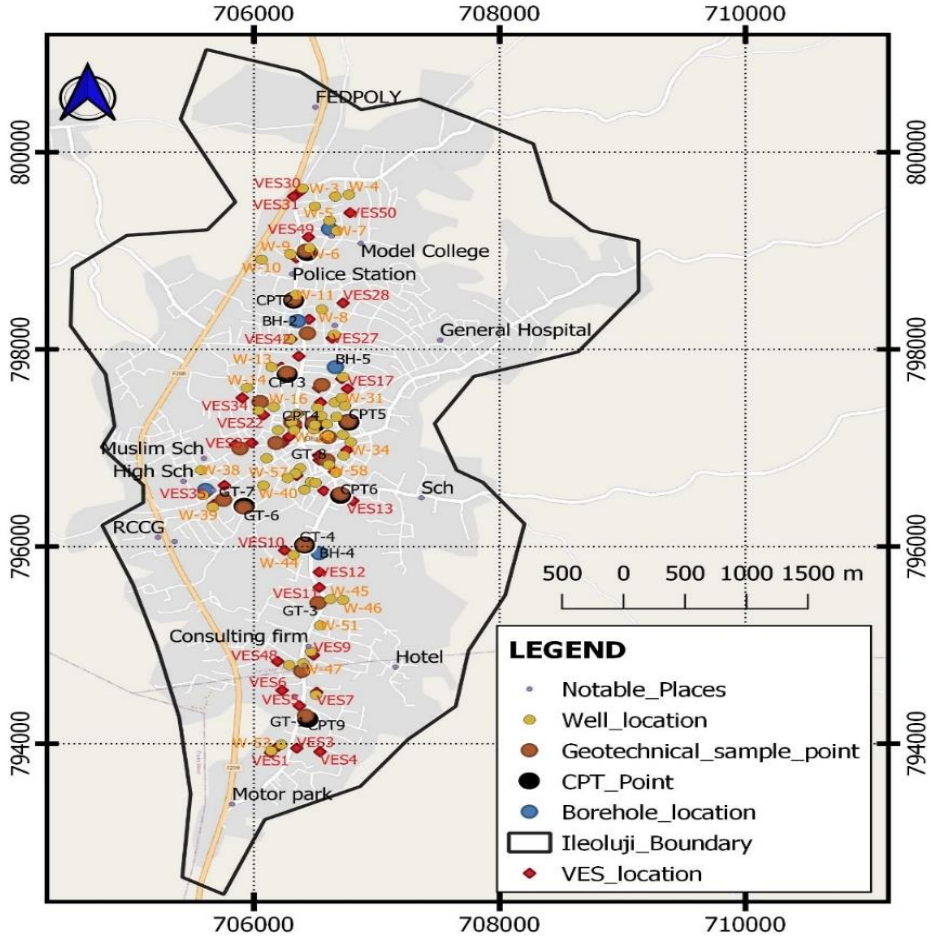

Fig. 3. Data Acquisition map for the study showing sample locations for geotechnical/geochemical and Field Survey

Magnetic method was also used, with measurements taken at 1 m interval along a traverse with GSN 8 Proton Precision Magnetometer. The field procedures was in line with Falowo et al. (2015). The distance covered for the survey was 500 m, on the same traverse established for the VES. Two sets of data were collected at each location and average determined, with sensor height at 1.5 m. The base station readings were taken before and after the data acquisition. The base station reading was used to correct the data for diurnal and offset corrections.

X-ray diffraction, differential temperature analysis, and a scanning electron microscopy are used to investigate the mineralogy and microstructure of the clay structure. The geochemical research in this work was carried out using X-ray diffraction. The determination of the water table level and any artesian pressure is an essential component of any ground study. The change of level or pressure over time may also necessitate decision. The water table level was found by gauging the depth to the water table in five boreholes after stabilization, and it is dependent on the permeability of their formations. As a result, measurements were made at regular periods until the water level became constant (Brassington, 1988). In addition to determining the chemical components in soil samples, which are the result of rock disintegration or erosion, or rock-water interaction. The chemical elements present in groundwater were not determined in this study, despite being an important aspect of engineering site investigation, particularly where salinity or the presence of corrosive effluents, such as sulphates and acidic waters, is suspected. Acid, bacteria, and oxidizing agents will affect steel foundation structures. These characteristics were not found in the water samples collected during the desk study/literature survey. Furthermore, firsthand interviews with town residents revealed a negative response to the aforementioned components. As a result, no water purity tests were performed. The static water level, hydraulic head measurement, and hydraulic conductivity, on the other hand, were found from fifty-five open wells and six boreholes.

Results: VES Technique

The summary of the VES is presented in Table 1, while a typical geologic section prepared for VESs 15, 19, 27, 28, and 45 in SW – NE direction, is shown in Figure 4. The curve types obtained from the study area varied from three layer curve (H), four layer curves (KH, HK, and QH), and five layer curve (HKH), and six layer curve (KHKH). The H curve type is the most preponderant (34 %) followed by KH (24 %), HKH (14 %), QH (14 %), HK (8 %), KHKH (6 %). This implies that the area is generally made of high resistive topsoil, underlain by high conductive weathered layer, and basement rock. From the Table 1, topsoil has resistivity ranging from 82 – 652 ohm-m (avg. 279 ohm-m) and thickness varying from 0.5 – 1.5 m (avg. 0.97 m) and composed of clay, sandy clay and clayey sand. The subsoil is characterized with resistivity ranging from 53 – 589 ohm-m (avg. 265 ohm-m) and have same composition as the topsoil, with thickness ranging from 2.1 to 10.5 m (avg. 5.20 m). The weathered layer has resistivity ranging between 38 ohm-m and 751 ohm-m (avg. 212 ohm-m), while resistivity range of 145 – 163 ohm-m is the most widespread (Figure 5a), and resistivity in the range of 38 – 145 ohm-m is extensive in the central part. These indicated a sandy clay weathered layer; the thickness ranged from 4.6 m and 38.7 m (avg. 17.5 m); while the spatial distribution map (Figure 5b) showed thickness range of 10 – 17 m being preponderant. The fractured basement/partly weathered/fresh basement has resistivity of 338 – 6550 ohm-m (avg. 1435 ohm-m), the depths to this rock varied from 9.9 – 39.6 m (avg. 22.4 m), while Figure 5c showed overburden thickness in the range of 13.5 to 24.1 m as most dominant, which can regard as moderate/thick weathering profile. Consequently, the topsoil, subsoil, and weathered layer are generally composed of sandy clay material, which can be regarded fairly competent soil material to support the civil engineering structures. Typical section shown in Figure 4 are characterized by topsoil (99 – 199 ohm-m), subsoil (302 – 413 ohm-m), weathered layer (84 – 251 ohm-m), fractured basement/partly weathered/fresh basement (398 – 3212 ohm-m). The relief of the basement is rugged.

Magnetic method

The relative magnetic field intensity along the profile (Figure 6) established for the geoelectric section showed amplitude variation of –17.60 nT to 16.85 nT (avg. 0.78 nT). This range of value is not unusual in basement complex, as similar values of -284 to 228 nT, -391 to 114 nT, -199 to 856 nT had been reported by Falowo et al. (2015). The profile showed relatively noisy anomaly, which can be considered as magnetically heterogeneous environment. However low magnetic anomalies observed are indication of structural features such as fracture, lineation, fault or joint system; this feature reflected on the geoelectric profile as fractured zone, while high magnetic values are reflection of magmatic intrusions, in form of dyke, sill, batholith, etc. Consequently, there is high degree of agreement between the magnetic and VES profiles.

Borehole Sections

The geologic units observed from the sites investigated (within migmatite, granite, and granite gneiss environments) comprised clay, sandy clay, clayey sand (which graded to sand or clayey material in many places), clay-sand mixture, and fresh basement rock (Figure 7). The thickness of the clay topsoil delineated under BHs-02 – 04 ranged from 1.1 – 5.7 m; the sandy clay was observed in all the boreholes with thickness range of 7.6 m (BH-03) to 23.2 m (BH-05); clayey sand has thickness variation of 1.2 m (BH-03) to 15.5 m (BH-04); clay-sand mixture has thickness varying from 3.3 m (BH-02) to 23.5 m (BH-03). The clay-sand mixture is the main water bearing units, which constitute the weathered layer. The depth to basement rock ranged between 33.8 – 44.1 m. The upper 10 m of the sections are dominated by clay, sandy clay, and clayey sand; while sandy clay being the most dominant soil. The SWL is deep ranging from 18.5 – 24.6 m. Thus this agreed with the VES result.

Hydrogeological Study

The hydrogeological investigation enables the prediction about the influence of groundwater system in civil engineering works. This can be carried out to assess location and thickness of water zone, their confinement, and hydrogeological margins; the levels of water and their variations with seasons (time); their storage potential and transmissivity; and their quality (Brassington, 1988). The data acquired from fifty-eight (58) open wells across different rocks (granite gneiss, granite, and migmatite) is presented in Table 2. The total depth of well investigated ranged from 6.5 – 15.1 m (avg. 10.1 m). The water column which is storage/reservoir potential of the wells ranged from 2.1 – 9.0 m (avg. 4.5 m) in migmatite rocks. The SWL varied from 2.5 m to 8.2 m (5.5 m), with corresponding hydraulic head of 246.1 – 267.8 m above the seal level (avg. 256.0 m). The information from the boreholes in Table 3, with total depth ranging from 38 0 – 48 m and an average of 42.4 m, showed SWL ranging from 19 – 26 m (avg. 21.8 m).

Geochemical Analysis

The stability and serviceability performance of soil for construction works is contingent upon the mineralogical make-up of the soil (Bell, 2007). The result of chemical analysis of selected mineral oxides contained in the soil samples, and silica-sesquioxide (S-S) ratio is presented in Table 4. They ranged from: MgO (0.19- 0.75 %, avg. 0.38), Al_2O_3 (15.66 – 24.5 %, avg. 18.45 %), SiO_2 (51.42 – 69.87 %, avg. 61.78), P_2O_5 (0 – 0.1 %, avg. 0.02 %), Na_2O (0.98 – 3.9 %, avg. 2.01 %), K_2O (0.23 – 4.52 %, avg. 2.45 %), CaO (0.82 – 0.27 %, avg. 0.07 %), TiO_2 (0.98 – 1.66 %, avg. 1.21 %), V_2O_5 (0.01 – 0.08 %, avg. 0.023 %), Cr_2O_3 (0 – 0.03 %, avg. 0.012 %), MnO (0.01 – 0.15 %, avg. 0.06 %), Fe_2O_3 (17.65 – 20.25 %, avg. 18.98 %), and CuO (0.01 – 0.03 %, avg. 0.02 %).

Table 1. VES Interpretation Results

East	North	Elev. (m)	VES NO.	Resistivity (Ohms-meter)						Thickness (m)					Depth (m)					Curve Type
				ρ_1	ρ_2	ρ_3	ρ_4	ρ_5	ρ_6	h_1	h_2	h_3	h_4	h_5	d_1	d_2	d_3	d_4	d_5	
706136	793908	256	1	458	201	1210				1.0	18.5				1	19.5				H
706199	793972	257	2	652	229	1003				0.6	16.5				0.6	17.1				H
706350	793953	256	3	428	112	994				0.8	22.6				0.8	23.4				H
706539	793917	259	4	329	85	778				0.8	17.9				0.8	18.7				H
706371	794384	266	5	201	470	110	885			1.1	5.9	29.5			1.1	7	36.5			KH
706230	794540	266	6	145	351	82	751			0.9	3.9	19.8			0.9	4.8	24.6			KH
706512	794521	267	7	102	315	108	898	217	1023	1.2	3.7	5.9	9.9	14.7	1.2	4.9	10.8	20.7	35.4	KHKH
706382	794714	266	8	551	99	614	225	898		0.8	6.3	4.6	18.1		0.8	7.1	11.7	29.8		HKH
706486	794897	260	9	361	523	188	858	91	1223	0.9	2.8	10.5	6.8	17.3	0.9	3.7	14.2	21	38.3	KHKH
706251	795960	262	10	233	357	65	1425			0.9	2.3	27.2			0.9	3.2	30.4			KH
706533	795584	264	11	189	421	147	1236			1.3	4.1	17.0			1.3	5.4	22.4			KH
706533	795740	265	12	345	72	1101				1.1	18.7				1.1	19.8				H
706805	796464	254	13	312	65	568				0.8	22.6				0.8	23.4				H
706659	796757	263	14	82	53	38	655			0.5	3.3	12.3			0.5	3.8	16.1			QH
706444	797243	259	15	99	413	118	3212			0.9	5.6	26.8			0.9	6.5	33.3			KH
706544	797462	252	16	128	520	213	1002			1.0	10.5	19.2			1	11.5	30.7			KH
706763	797600	256	17	241	158	92	998			1.2	5.7	14.4			1.2	6.9	21.3			QH
706716	797701	256	18	305	193	102	689			1.2	6.3	17.9			1.2	7.5	25.4			QH
706528	797609	252	19	187	410	251	1356			0.6	4.0	13.5			0.6	4.6	18.1			KH
706288	797114	268	20	201	88	806				0.9	20.5				0.9	21.4				H
706235	797050	269	21	362	132	1455				0.8	16.8				0.8	17.6				H
706079	797334	257	22	446	144	521	97	936		0.8	2.1	9.8	16.2		0.8	2.9	12.7	28.9		HKH
706356	797343	252	23	354	222	751	123	1330		0.9	3.3	12.3	15.7		0.9	4.2	16.5	32.2		HKH
706361	797233	262	24	319	195	470	122	1114		0.9	2.9	7.7	16.8		0.9	3.8	11.5	28.3		HKH
706366	797930	259	25	229	87	999				0.8	23.2				0.8	24				H
706225	797820	255	26	310	45	1652				1.2	16.5				1.2	17.7				H
706638	798113	264	27	199	84	2356				1.4	18.7				1.4	20.1				H
706727	**798470**	263	28	175	302	201	852			1.1	6.3	18.9			1.1	7.4	26.3			KH
706450	798305	267	29	502	322	612	108	1232		0.9	3.8	10.3	14.8		0.9	4.7	15	29.8		HKH
706382	799606	272	30	156	98	57	911			0.6	6.9	18.5			0.6	7.5	26			QH
706324	799551	269	31	195	120	68	1102			0.9	7.1	19.6			0.9	8	27.6			QH
706345	798928	260	32	314	132	458	110	2250		1.2	2.5	8.9	19.4		1.2	3.7	12.6	32		HKH
706350	798498	258	33	445	80	2378				1.1	18.2				1.1	19.3				H
705906	797508	255	34	329	89	1468				1.3	23.4				1.3	24.7				H
705613	796537	258	35	498	120	877				0.9	22.2				0.9	23.1				H
705760	796620	259	36	214	403	182	2444			1.1	7.4	18.3			1.1	8.5	26.8			KH
705984	797050	261	37	205	81	801				0.8	22.5				0.8	23.3				H
705849	797032	258	38	222	419	90	3358			1.4	5.4	19.2			1.4	6.8	26			KH
705896	796409	259	39	474	221	6550				0.5	15.5				0.5	16				H

Table 1 continued

East	North	Elev. (m)	VES NO.	Resistivity (Ohmns-meter)						Thickness (m)					Depth (m)					Curve Type
				ρ_1	ρ_2	ρ_3	ρ_4	ρ_5	ρ_6	h_1	h_2	h_3	h_4	h_5	d_1	d_2	d_3	d_4	d_5	
705676	796427	258	40	188	369	102	1616			0.8	3.4	13.7			0.8	4.2	17.9			KH
706758	796977	266	41	112	589	174	4122			1.5	2.2	9.8			1.5	3.7	13.5			KH
706303	798104	265	42	477	214	509	115	2750		1.1	8.8	19.4			1.1	9.9	29.3			HKH
706434	796015	261	43	94	218	144	998	58	3696	1.3	7.7	12.3	8.2	13.8	1.3	9	21.3	29.5	43.3	KHKH
706570	796565	258	44	232	152	93	750			0.7	6.9	18.6			0.7	7.6	26.2			QH
706350	796720	267	45	168	85	445	398			0.9	6.9	13.4			0.9	7.8	21.2			HK
706533	796876	274	46	86	45	690				0.9	38.7				0.9	39.6				H
706528	796922	274	47	314	112	555	410			1.1	9.9	19.2			1.1	11	30.2			HK
706194	794833	262	48	186	92	480	338			1.2	5.4	18.7			1.2	6.6	25.3			HK
706444	799139	267	49	411	147	621	448			1.2	3.6	14.9			1.2	4.8	19.7			HK
706784	799386	269	50	159	121	94	661			0.8	3.3	21.2			0.8	4.1	25.3			QH

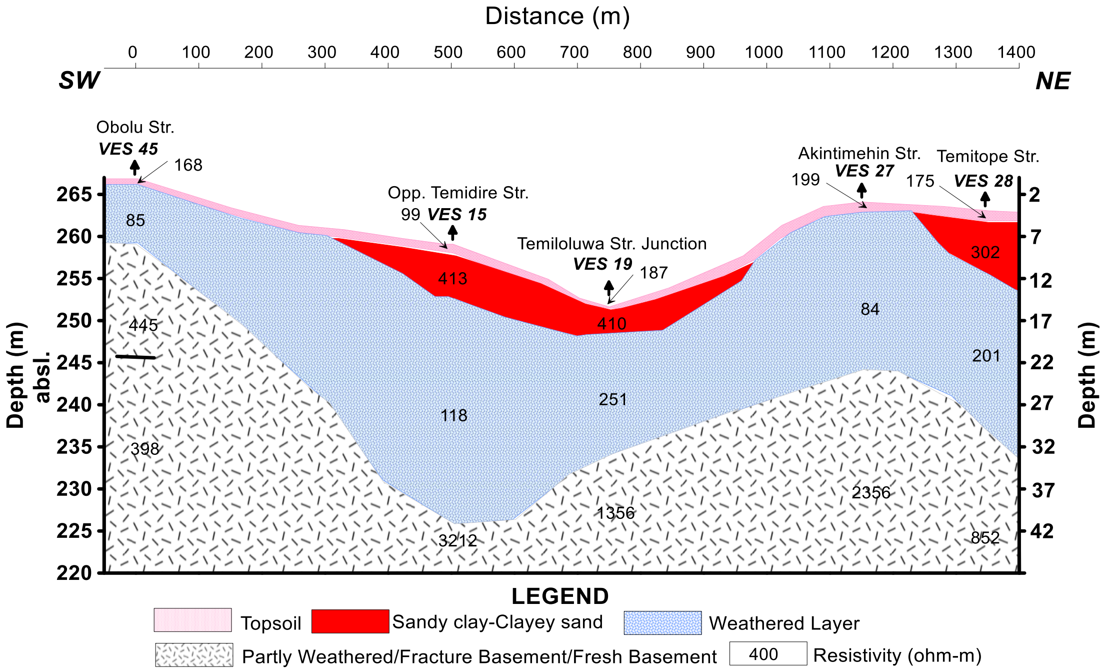

Fig. 4. Geologic Section/Profile along the selected VES point established in the study area

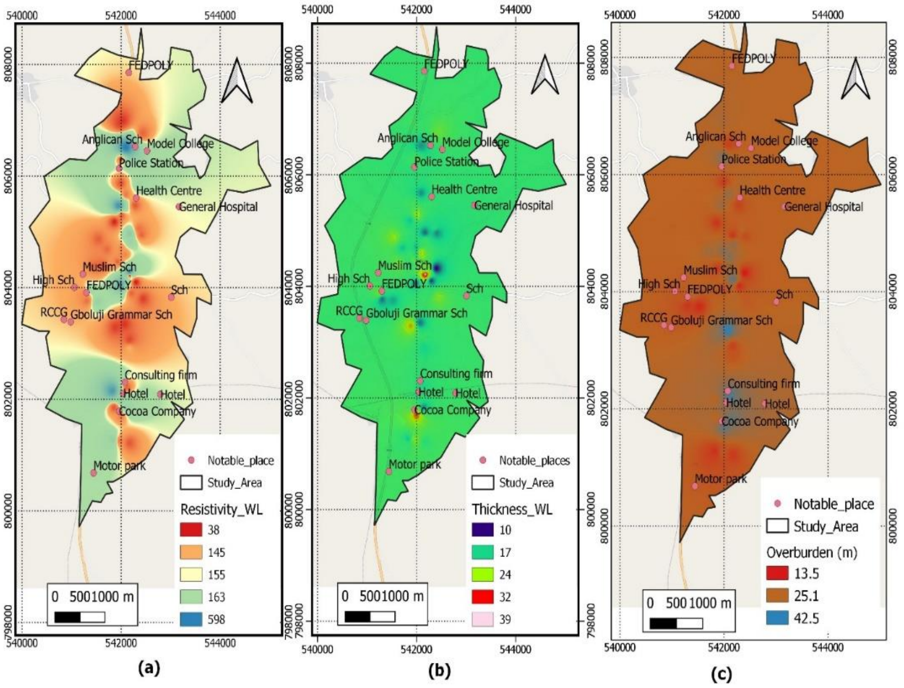

Fig. 5. Spatial Distribution Map of (a) weathered layer resistivity (b) weathered layer thickness (c) overburden thickness across the study area

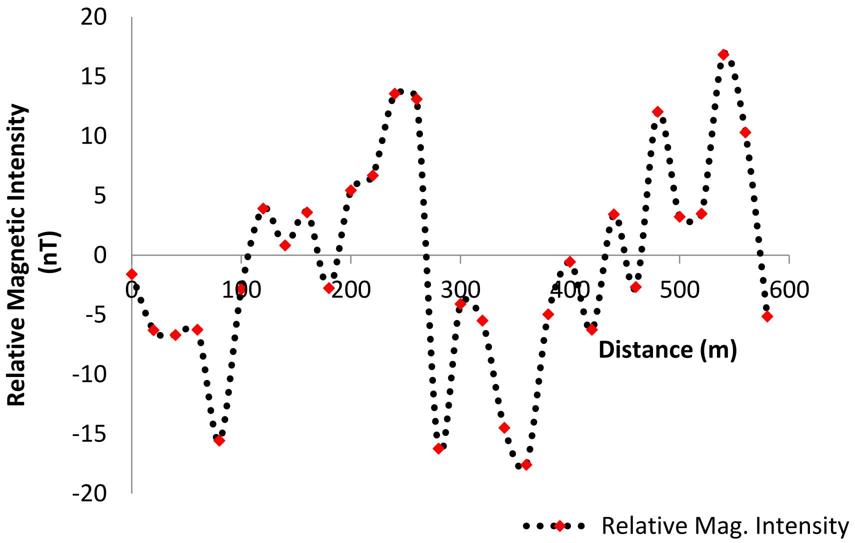

Fig. 6. Magnetic Profile across VESs 15, 19, and 45

Consequently, the soil is abundantly rich in SiO_2, Fe_2O_3, and Al_2O_3, with the concentration of SiO_2 more than combined concentrations of other mineral oxides. This indicates that parent rock material in the study is silica-rich igneous rock, suggestive of granite, gneiss, rhyolite, dacite, granodiorite, diorite, andesite, quartz, and orthoclase porphyries. However, this is inconformity with geological observation of granite, granite-gneiss, and migmatite dominating the environment. The S-S ratio varied between 1.39 – 1.97 (avg. 1.66). Accordingly, the soils' S-S ratio is within lateritic type range of 1.33 – 2.0 (Martin and Doyne, 1927).

Geotechnical Analysis

The geotechnical results for the sampled soils are presented in Tables 5-7. The natural moisture content varied from 15.5 to 20.2 % (avg. 18.33 %), this range is above the 5 – 15 % acceptable range favourable for civil engineering uses. Grain size analysis can be used to characterize the subsoil material for engineering works, which can serve as a guide to the engineering performance of the soil type and also provides a means by which soils can be identified quickly. The sand content ranged from 30.5 – 67.8 % (avg. 44.8 %), % silt and clay contents ranged from 8.9 to 17.2 % (avg. 12.7 %) and 17.1 to 58.3 % (avg. 33.85 %) respectively.

The %fines ranged from 32.2 to 69.5 (avg. 57.5). The composition of the soil is dominated (in order of magnitude) by clay, sand, and silt. The amount of %fines recorded is more than 35 % specification of Nigerian federal ministry of works and housing (FMWH, 1997).

The plasticity chart (Figure 8a) shows that the samples are dominated by clay of low (75 %) to high (25 %) plasticity/compressibility. In addition, 65 % of the soil samples plotted above the A-line. In terms of clay mineralogy, the soil samples are plotted dominantly within the boundary of illite (Figure 8b). Illite has a similar structure similar to montmorillonite, however in illite the interlayers are bonded together with a potassium ion linkage, making it to have relatively less attraction for water (Bell, 2007). The activity ranged from 0.32 to 0.88 (avg. 0.48) signifying inactive clay type (Bell, 2007). The specific gravity (SG) is closely related with soil's mineralogy and/or chemical contents; the higher SG, the higher the degree of laterization. In addition, the larger the clay fraction and alumina contents, the lower is the SG. The values of specific gravity of the samples ranged between 2.66 – 2.73 (avg. 2.70). The standard range of value of specific gravity of soils lies between 2.60 and 2.80, these values are considered normal for construction works.

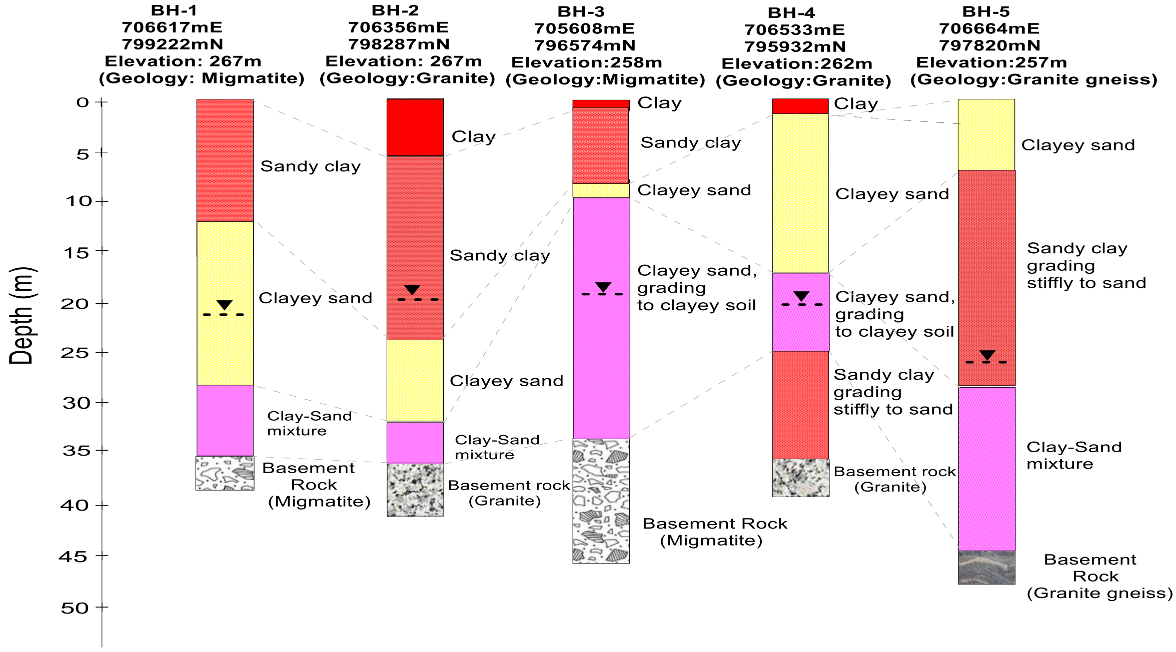

Fig. 7. The borehole sections across the study area, in granite, migmatite and granite gneiss environments

The liquid limit (LL) values ranged between 34.2 to 59.2 % (avg. 47.99 %), plastic limits (PL) ranged between 19.2 to 40.6 % (avg. 27.79 %) and plasticity index (PI) is between 15.0 to 24.9 % (avg. 20.21 %). Soil with high LL, PL, and PI are usually characterized with low bearing pressure. This implies high plasticity soil, with low expansive and marginal degree of severity (IS: 1494). The linear shrinkage ranged between 8.8 to 12.8 % (avg. 10.4 %), signifying a medium swelling potential. The group index (GI) values obtained ranged from 1 to 11 (avg. 6) corresponding to fair subgrade soil (George and Uddin, 2000). The unit weight of the soils varied from 18.5 – 22.32 KN/m^3 (avg. 19.99 KN/m^3), cohesion of 30.6 – 69.8 KN/m^2 (avg. 48.41 KN/m^2), and angle of friction of 11.6 – 26.8° (avg. 17.41°).

The unconfined compressive strength (UCS) ranged from 138.7– 231.2 KN/m2 (avg. 186.78 KN/m2). The hydraulic conductivity of the samples is between 1.15E-07 to 3.66E-06 cm/s (avg. 2.13E-06 cm/s) indicative of poor drainage condition as per BIS. The maximum dry density (MDD) for the soil samples varied between 1843 and 2161 kg/m^3 (avg. 1980 kg/m^3) at standard proctor compaction energy while the optimum moisture content (OMC) ranged between 10.4 and 18.5 % (avg. 14.77 %). All the soil samples have high MDD at moderately low OMC.

The California Bearing Ratio (CBR) is an empirical test employed in road engineering as an index of compacted material strength and rigidity, corresponding to a defined level of compaction. All compacted samples show soaked and un-soaked CBR values ranging between 4 and 13 % (avg. 7 %) and 42 – 81 % (avg. 59 %) respectively. The consolidation characteristics of the soils showed coefficient of consolidation (C_v) (0.007 – 0.0169 m^2/yr; avg. 0.0113 m^2/yr), coefficient of compressibility (a_v) (0.1114 – 0.2995 MPa^{-1}; avg. 0.2365 MPa^{-1}), coefficient of volume compressibility (M_v) (0.10976 – 0.24566 m^2/KN; avg. 0.204064 m^2/KN), compression index (C_C) (0.03437 – 0.0178; avg. 0.0443), swelling index (C_S) (-0.00653 to -0.00302; avg. -0.00378), recompression index (C_r) (0.011 – 0.029; avg. 0.0216) and void ratio (e_o) (0.12 – 0.58; avg. 0.292632). The preconsolidation pressure applied was 0.040 MPa. Consequently, using the averages of all the consolidation parameters, based on C_c the soils are hard clay with high degree of compressibility i.e. C_c range of 0.3 – 0.15; based on M_v the soils are expected to exhibit medium degree of compressibility typical of varved and laminated clays or firm to stiff clays (0.25 – 0.125 m^2/KN). The coefficient of consolidation is the indicative of the combined effect of compressibility and permeability of soil on the rate of volume change (Upadhyay, 2015).

CPT Analysis

The results of the CPT is presented in Table 8, while the plotted sounding curves for the nine locations is shown in Figure 9 showing the cone resistance (Q_c), sleeve resistance (S_r), friction ratio (F_R), allowable bearing capacity (Q_{all}), and Modulus Number (M-number) with depth. The obtained values of Q_c ranged from 12 – 142 kg/cm^2 (avg. 74 kg/cm^2), S_r varied from 43 – 523 kg/cm^2 (avg. 220 kg/cm^2), Q_{cn} is between 34 - 365 kg/cm^2 (avg. 199 kg/cm^2), F_R ranged from 1.94 – 4.84 (avg. 3.11), Q_{all} varied from 27.44 – 297.68 KN/m^2 (avg. 162.56 KN/m^2), UCS is in between 4.85 – 54.52 KN/m^2 (avg. 29.52 KN/m^2), C_u ranged from 2.42 – 27.26 KN/m^2 (avg. 14.76 KN/m^2), M-number varied from 7 – 74 (avg. 40), E_{square} is between 206 – 2232 KN/m^2 (avg. 1219 KN/m^2), E_{strip} ranged from 288 - 3126 KN/m^2 (avg. 1707 KN/m^2), N_{cor} varied from 3 -36 (avg. 19), and σ_o is between 4.63 – 40.7 KN/m^3 (avg. 15.4 KN/m^3). The allowable bearing pressure for strip (Q_{strip}) and square (Q_{square}) ranged from 373 – 3399 KN/m^2 (avg. 1886 KN/m^2), and 537 - 4212 KN/m^2 (avg. 2374 KN/m^2) respectively.

The geologic units showed for CPT 1 (0 - 0.5 m: clay silt to silty clay; 0.5 – 0.75 m: sandy silt to clayey silt; 0.75 – 1.0 m: silty sand to sandy silt); CPT 2 (0 - 0.5 m: clay silt to silty clay; 0.5 – 0.75 m: sandy silt to clayey silt; 0.75 – 0.8 m: silty sand to sandy silt); CPT 3 (0 – 0.75 m: clay silt to silty clay; 0.75 – 1.0 m: silty sand to sandy silt); CPT 4 (0 - 0.5 m: silty clay to clay; 0.5 – 0.75 m: clayey silt to silty clay; 0.75 – 1.0 m: sandy silt to clayey silt; 1.0 – 1.25 m: silty sand to sandy silt; 1.25 – 1.50 m: sand to silty sand); CPT 5 (0 – 0.75 m: sandy silt to clayey silt; 0.75 – 1.0 m: silty sand to sandy silt; 1.0 – 1.2 m: sand to silty sand; 1.2 – 1.25: silty sand to sandy silt); CPT 6 (0 – 0.5 m: clayey silt to silty clay; 0.5 – 1.0 m: sandy silt to clayey silt; 1.0 – 1.5 m: silty sand to sandy silt; 1.5 – 1.75 m: sandy silt to clayey silt); CPT 7 (0 – 0.5 m: clay; 0.5 – 1.75 m: clayey silt to silty clay; 1.75 – 1.90 m: sandy silt to clayey silt; 1.9 – 2.0 m: very stiff fine grained clayey soil); CPT 8 (0 – 0.5 m: clay; 0.5 – 0.75 m: silty clay to clay; 0.75 – 1.90 m: clayey silt to silty clay; 1.90 – 2.0 m: sandy silt to clayey silt); CPT 9 (0 – 0.5 m: clay; 0.5 – 0.75 m: silty clay to clay; 0.75 – 1.0 m: clayey silt to silty clay; 1.0 – 1.2 m: sandy silt to clayey silt; 1.2 – 1.25 m: silty sand to sandy silt).

Consequently, the soil, the soil is of fine grained in the upper 2.0 m with dominant clayey silt to silty clay, and sandy silt to clayey silt, which is usually regarded as weak soil zone for most civil engineering construction. This agreed with the result of the VES, borehole sections, and grain size distribution, which identified the topsoil/subsoil as sandy clay/clay sand. The average Q_c (74 kg/cm^2), Q_{all} of 163 KN/m^2 obtained can support light/medium weight foundation structure without excessive settlement. The refusal depths for the survey varied between 1 – 2.0 m, and are usually terminated in silty sand to sandy silt and sandy silt to clayey silt. Using the values of C_U of the soils (avg. 14.76 kg/m^2), the consistency of the soils is in between soft to firm. From the graph, the Q_C, M-Number, and Q_{all} increase with depth.

Table 2. Summary of the well information obtained from fifty-eight open wells during the wet season

East	North	Well. No	Elevation (m)	Total Depth	SWL	Water Column (m)	Hydraulic Head (m)	Geology
706397	799634	W-1	272	8.2	4.5	3.7	267.5	Granite
706497	799451	W-2/VES 49	269	12.3	7.5	4.8	261.5	Granite
706664	799551	W-3	271	14.5	8.2	6.3	262.8	Granite
706774	799570	W-4/VES50	271	6.5	3.2	3.3	267.8	Granite
706617	799304	W-5	268	9.5	5.5	4	262.5	Granite
706455	799029	W-6	266	8.7	3.9	4.8	262.1	Granite
706674	799203	W-7	267	10.4	6.2	4.2	260.8	Granite
706554	798406	W-8	263	12.7	5.8	6.9	257.2	Granite
706298	798965	W-9	261	9.8	6.3	3.5	254.7	Granite
706063	798910	W-10	258	7.8	4.3	3.5	253.7	Granite
706340	798553	W-11	256	13.3	5.6	7.7	250.4	Granite
706293	798104	W-12/VES 25	264	15.1	8.2	6.9	255.8	Granite
706146	797820	W-13	255	8.6	5.2	3.4	249.8	Granite Gneiss
705943	797609	W-14	255	9.5	3.7	5.8	251.3	Granite
706037	797380	W-15/VES 37	256	8.2	5.3	2.9	250.7	Granite
706162	797417	W-16	254	12.2	6.8	5.4	247.2	Migmatite
706350	797343	W-17/VES 20	252	14.6	5.6	9	246.4	Migmatite
706309	797261	W-18/VES 21	259	8.8	2.5	6.3	256.5	Migmatite
706329	797178	W-19	266	6.7	3.4	3.3	262.6	Granite Gneiss
706199	797178	W-20	263	11.3	7.2	4.1	255.8	Granite Gneiss
706654	798150	W-21	265	14.9	6.8	8.1	258.2	Granite Gneiss
706518	797407	W-22	252	9.2	3.8	5.4	248.2	Granite Gneiss
706727	797719	W-23/VES 17	256	8.0	5.5	2.5	250.5	Granite Gneiss
706486	797188	W-24	262	11.4	7.4	4	254.6	Granite Gneiss
706497	797233	W-25	259	9.6	5.2	4.4	253.8	Granite Gneiss
706549	797325	W-26	255	7.4	3.6	3.8	251.4	Granite Gneiss
706659	797462	W-27	254	12.8	7.9	4.9	246.1	Granite Gneiss
706716	797508	W-28	255	10.9	6.5	4.4	248.5	Migmatite
706596	797243	W-29	259	13.3	8.1	5.2	250.9	Migmatite
706674	797316	W-30	257	8.5	4.4	4.1	252.6	Migmatite
706742	797426	W-31	256	9.9	3.6	6.3	252.4	Migmatite
706606	797123	W-32	264	8.7	3.5	5.2	260.5	Migmatite
706727	797133	W-33	263	9.2	5.2	4	257.8	Migmatite
706789	797059	W-34	263	8.6	4.3	4.3	258.7	Granite
706732	796922	W-35/VES 14	268	9.7	6.5	3.2	261.5	Granite

706669	796748	W-36	262	10.7	6.9	3.8	255.1	Granite
705587	796519	W-37	257	8.7	3.3	5.4	253.7	Granite
705571	796775	W-38/VES 35	257	6.5	4.0	2.5	253	Migmatite
705666	796400	W-39	257	9.8	4.9	4.9	252.1	Granite
706079	796620	W-40	257	10.8	7.2	3.6	249.8	Granite
706413	796574	W-41/VES 33	261	7.7	4.6	3.1	256.4	Granite Gneiss
706465	796656	W-42	264	9.5	4.8	4.7	259.2	Granite
706502	796647	W-43	263	10.5	5.6	4.9	257.4	Migmatite
706324	795914	W-44/VES 8	263	12.3	7.7	4.6	255.3	Migmatite
706622	795465	W-45/VES 9	265	9.4	6.2	3.2	258.8	Migmatite
706727	795456	W-46/VES 32	264	7.6	5.5	2.1	258.5	Migmatite
706403	794815	W-47	262	8.9	3.9	5	258.1	Granite Gneiss
706288	794796	W-48/VES 6	263	13.8	7.9	5.9	255.1	Granite Gneiss
706507	794494	W-49	267	11.5	6.6	4.9	260.4	Granite Gneiss
706465	794934	W-50	259	12.6	8.1	4.5	250.9	Granite Gneiss
706539	795199	W-51	264	10.2	5.8	4.4	258.2	Granite Gneiss
706225	793990	W-52/VES 44	257	8.5	4.7	3.8	252.3	Granite Gneiss
706141	793926	W-53	257	8.9	6.2	2.7	250.8	Granite Gneiss
706105	796894	W-54	265	9.0	6.1	2.9	258.9	Granite Gneiss
706376	796794	W-55	270	8.5	4.2	4.3	265.8	Granite Gneiss
706340	796739	W-56	267	10.5	5.9	4.6	261.1	Granite Gneiss
706277	796693	W-57	264	8.7	4.7	4	259.3	Granite
706612	796830	W-58	270	7.6	3.8	3.8	266.2	Granite

Table 3. Borehole Information obtained from six boreholes

East	North	Borehole No.	Elevation (m)	Total Depth (m)	SWL (m)	Geology	Present State
706617	799222	BH-1	267	38	22	Granite	Functioning
706356	798287	BH-2	267	42	19	Granite	Functioning
705608	796574	BH-3	258	45	22	Gneiss	Functioning
706533	795932	BH-4	262	39	20	Gneiss	Functioning
706664	797820	BH-5	257	48	26	Granite	Functioning

Table 4. Result of the chemical analysis of selected mineral oxide

Sample No.	MgO	Al_2O_3	$Si0_2$	P_2O_5	Na_2O	k_2O	CaO	$Ti0_2$	V_2O_5	Cr_2O_3	MnO	Fe_2O_3	CuO	S-S Ratio	Class
IL-1	0.23	17.56	62.2	0.01	2.29	4.52	0.32	1.66	0.01	0.01	0.03	19.65	0.03	1.67	Lateritic
IL-2	0.33	19.98	63.5	0.01	3.25	3.4	0.22	1.45	0.01	0.01	0.03	18.23	0.01	1.66	Lateritic
IL-3	0.38	24.5	60.5	0.01	3.22	0.23	0.35	1.28	0.03	0.01	0.03	18.95	0.03	1.39	Lateritic
IL-4	0.65	18.38	59.88	0.01	1.02	0.56	0.82	1.25	0.02	0.01	0.03	18.66	0.01	1.62	Lateritic
IL-5	0.19	18.96	61.25	0.01	1.2	1.87	0.21	1.22	0.04	0.01	0.03	17.65	0.01	1.67	Lateritic
IL-6	0.42	17.25	58.95	0	0.98	3.05	0.25	1.32	0.03	0.02	0.05	18.27	0.02	1.66	Lateritic
IL-7	0.33	18.23	63.21	0	1.45	2.54	0.18	1.12	0.02	0.01	0.03	19.88	0.01	1.66	Lateritic
IL-8	0.23	17.22	69.8	0	3.25	2.32	0.24	1.04	0.01	0.01	0.01	18.24	0.01	1.97	Lateritic
IL-9	0.52	18.45	57.45	0	2.45	2.45	0.19	1.11	0.01	0.01	0.03	19.59	0.01	1.51	Lateritic
IL-10	0.47	15.66	60.2	0.01	3.1	3.36	0.22	1.15	0.02	0.01	0.12	19.22	0.03	1.73	Lateritic
IL-11	0.56	17.85	60.58	0	1.45	1.26	0.17	0.98	0.03	0.01	0.15	18.66	0.03	1.66	Lateritic
IL-12	0.31	17.65	65.87	0	3.9	3.65	0.21	1.02	0.01	0.01	0.03	17.73	0.01	1.86	Lateritic
IL-13	0.39	18.95	69.87	0	2.44	1.39	0.18	0.99	0.01	0.02	0.15	20.1	0.02	1.79	Lateritic
IL-14	0.75	17.7	63.23	0.01	1.02	1.45	0.63	1.24	0.08	0.03	0.03	19.46	0.01	1.70	Lateritic
IL-15	0.22	18.95	60.22	0.1	1.54	2.65	0.23	1.11	0.02	0.01	0.15	20.25	0.03	1.54	Lateritic
IL-16	0.42	19.2	64.1	0.1	1.2	2.59	0.21	1.09	0.02	0.01	0.03	18.63	0.01	1.69	Lateritic
IL-17	0.31	19.52	60.1	0.01	2.22	2.68	0.19	1.44	0.01	0.02	0.03	18.57	0.01	1.58	Lateritic
IL-18	0.31	17.74	63.32	0.01	1.65	2.53	0.07	1.23	0.03	0.01	0.13	19.25	0.01	1.71	Lateritic

IL-19	0.24	16.69	59.95	0.01	1.2	3.58	0.12	1.43	0.02	0	0.03	20.13	0.03	1.63	Lateritic
IL-20	0.29	18.5	51.42	0.01	1.26	2.9	0.47	1.08	0.03	0.01	0.15	18.45	0.02	1.39	Lateritic

Table 5: Summary of Geotechnical Analysis showing the particle size distribution, Consistency limit and soil classification

Sample No.	Location		Elev. (m)	NMC (%)	Grain size Distribution				SG	Consistency Limits			SL	Group Index	AASHTO Class	USCS Class
	Easting (m)	Northing (m)			% Sand	% silt	% Clay	% Fines		PL (%)	LL (%)	PI (%)				
IL-1	706421	794283	263	18.4	52.3	17.2	30.5	47.7	2.68	22.1	43.3	21.2	9.6	2	A-7-6	CL
IL-2	706390	794737	265	18.7	37.1	17.1	45.8	62.90	2.72	23.4	48.3	24.9	9.1	8	A-7-6	CL
IL-3	706523	795428	265	17.1	67.8	15.1	17.1	32.2	2.66	19.2	34.2	15.0	10.6	1	A-2-4	CL
IL-4	706410	796015	261	18.5	40.2	10.2	49.6	59.80	2.68	29.6	48.8	19.2	9.8	1	A-7-5	ML
IL-5	706708	796537	254	18.9	38.5	11.3	50.2	61.5	2.69	35.7	54.3	18.6	11.5	1	A-7-5	MH
IL-6	705919	796395	259	17.7	32.6	9.8	57.6	67.40	2.71	30.7	49.3	18.6	9.2	2	A-7-5	ML
IL-7	705754	796473	260	19.5	52.3	12.3	35.4	47.7	2.67	24.5	44.0	19.5	12.3	9	A-7-6	CL
IL-8	706593	796876	273	18.3	42.5	12.4	45.1	57.50	2.70	27	47.2	20.2	11.5	4	A-7-6	CL
IL-9	706606	797110	265	15.5	50.2	15.3	34.5	49.8	2.70	21.3	42.9	21.6	10.1	1	A-7-6	CL
IL-10	706769	797270	259	19.1	39.8	9.2	51	60.20	2.72	27.8	47.6	19.8	9.9	7	A-7-6	CL
IL-11	706486	797256	258	18.4	37.5	11.8	50.7	62.5	2.72	34.8	55.1	20.3	11.6	7	A-7-5	MH
IL-12	706052	797467	255	20.2	48.2	12.6	39.2	51.80	2.69	24.9	43.6	18.7	9.0	8	A-7-6	CL
IL-13	706180	797050	267	19.7	32.2	10.2	57.6	67.8	2.71	29.2	48.5	19.3	10.2	5	A-7-5	ML
IL-14	705888	796995	258	18.2	34.7	16.3	49	65.30	2.72	26.8	48.3	21.5	8.8	4	A-7-6	CL
IL-15	706269	797765	253	17.5	30.5	15.9	53.6	69.5	2.73	26.7	49.5	22.8	10.9	9	A-7-6	CL
IL-16	706554	797641	252	18.6	36.8	12.4	50.8	63.20	2.72	40.6	59.2	18.6	12.8	9	A-7-5	MH
IL-17	706437	798163	268	18.0	56.4	12.2	31.4	43.6	2.69	21.6	41.0	19.4	10.2	11	A-6-5	CL
IL-18	706322	798507	257	16.3	37.7	14.6	47.7	62.30	2.71	32.9	55.4	22.5	9.5	7	A-7-6	MH
IL-19	706421	799002	265	19.5	49.9	9.7	40.4	50.1	2.72	22.7	42.5	19.8	12.3	10	A-7-5	CL
IL-20	706309	797261	259	18.5	32.8	8.9	58.3	67.20	2.70	34.2	56.8	22.6	9.7	6	A-7-6	MH

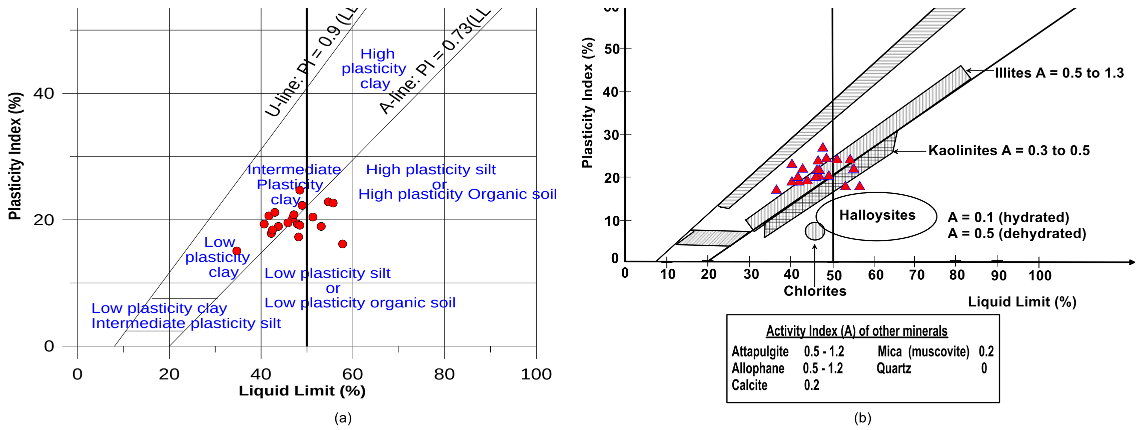

Fig. 8. (a) Plasticity Chart for the soil samples, showing prominent CL and CI plasticity group (b) Clay mineralogy group of the soil samples with most within Illite group

Table 6. Summary of Geotechnical Analysis showing the grading curve properties, CBR, cohesion, and consolidation parameters

Sample No.	Unit Weight (KN/m^3)	Triaxial Test		UCS (KPa)	K (cm/s)	Clay Mineralogy	Activity	
		Cohesion (KN/m^2)	Angle of friction (°)				Values	Soil Type
IL-1	20.98	58.6	17.2	206.5	4.07E-07	I-M	0.70	Inactive
IL-2	19.88	69.8	16.4	231.2	1.15E-07	I-M	0.54	Inactive
IL-3	21.62	35.8	16.4	138.7	2.49E-06	I-M	0.88	Normal
IL-4	19.67	51.3	15.5	196.2	1.50E-06	I	0.39	Inactive
IL-5	18.87	45.8	18.6	188.4	2.34E-06	K	0.37	Inactive
IL-6	18.69	36.6	17.8	163.5	2.52E-06	I	0.32	Inactive
IL-7	20.35	38.5	18.3	156.9	1.96E-06	I	0.55	Inactive
IL-8	19.50	30.6	16.4	179.2	2.24E-06	I	0.45	Inactive
IL-9	20.32	40.2	20.6	169.8	1.26E-06	M-I	0.63	Inactive
IL-10	18.63	52.6	16.4	186.5	1.89E-06	I	0.39	Inactive
IL-11	19.47	62.3	18.9	201.2	2.15E-06	K	0.40	Inactive
IL-12	18.60	36.9	17.8	167.5	2.65E-06	I	0.48	Inactive
IL-13	22.32	38.7	13.6	178.2	2.02E-06	I	0.34	Inactive
IL-14	20.75	42.8	11.6	180.1	2.78E-06	I-M	0.44	Inactive
IL-15	20.25	54.5	12.2	194.3	1.49E-06	I-M	0.43	Inactive
IL-16	18.50	63.5	15.3	211.6	3.66E-06	K-H	0.37	Inactive
IL-17	19.80	58.6	22.4	204.2	2.97E-06	I-M	0.62	Inactive
IL-18	20.68	48.9	14.6	198.7	3.01E-06	I	0.47	Inactive
IL-19	21.20	39.8	26.8	178.4	2.14E-06	I	0.49	Inactive
IL-20	19.64	62.4	21.4	204.5	3.10E-06	I	0.39	Inactive

Table 7. Compaction characteristics, CBR, and Consolidation tests conducted on the soil samples

Sample No.	MDD Kg/m^3	OMC	CBR soaked	CBR unsoaked	C_v (m^2/yr)	a_v MPa^{-1}	m_v MPa^{-1}	σ_p MPa	C_c Index	C_s	C_r	e_o
IL-1	2099	13.5	8	57	0.0112	0.2521	0.20830	0.0400	0.0333	-0.00365	0.024	0.263
IL-2	1988	17.6	4	42	0.0095	0.2926	0.22927	0.0400	0.0386	-0.00319	0.028	0.276
IL-3	2161	11.1	13	81	0.0122	0.1321	0.10976	0.0400	0.0178	-0.00653	0.013	0.204
IL-4	1985	18.5	7	44	0.0070	0.2995	0.24450	0.0400	0.0349	-0.00315	0.025	0.264
IL-5	1986	17.6	6	49	0.0122	0.2334	0.21212	0.0400	0.0399	-0.00311	0.021	0.581
IL-6	1954	15.8	6	53	0.0111	0.2885	0.23316	0.0400	0.0354	-0.00302	0.024	0.465
IL-7	1889	17.7	4	54	0.00875	0.2774	0.22440	0.0400	0.0306	-0.00331	0.027	0.326
IL-8	1986	17.2	4	49	0.0124	0.2863	0.20007	0.0400	0.0335	-0.00355	0.018	0.325
IL-9	2121	13.1	10	78	0.0103	0.1120	0.11985	0.0400	0.0296	-0.00612	0.020	0.132
IL-10	1988	13.5	6	60	0.0121	0.2462	0.23360	0.0400	0.0338	-0.00360	0.019	0.360
IL-11	1892	15.8	6	71	0.0107	0.2112	0.16555	0.0400	0.0406	-0.00307	0.023	0.274
IL-12	1856	14.6	8	60	0.0098	0.2601	0.23341	0.0400	0.0302	-0.00333	0.020	0.281
IL-13	1843	17.5	5	58	0.0090	0.2568	0.24566	0.0400	0.0347	-0.00344	0.024	0.263
IL-14	1965	14.8	7	68	0.0126	0.2469	0.22146	0.0400	0.0345	-0.00326	0.025	0.199
IL-15	1930	14.5	4	70	0.0144	0.2501	0.21482	0.0400	0.0355	-0.00411	0.022	0.255
IL-16	1972	13.3	7	65	0.0169	0.2423	0.16678	0.0400	0.0443	-0.00326	0.024	0..451
IL-17	2002	14.8	11	49	0.0110	0.1114	0.17854	0.0400	0.0279	-0.00333	0.012	0.120
IL-18	1991	11.4	5	55	0.0101	0.2489	0.20693	0.0400	0.0409	-0.00398	0.029	0.326
IL-19	2102	12.6	13	79	0.0125	0.2354	0.19975	0.0400	0.0293	-0.00502	0.011	0.222
IL-20	1896	10.4	6	43	0.0115	0.2459	0.23334	0.0400	0.0421	-0.00362	0.023	0.424

C_v – coefficient of consolidation
a_v – Coefficient of compressibility
m_v – Coefficient of Vol. compressibility
σ_p – Preconsolidation pressure
C_c – Compression index
C_s – Swelling index
C_r – Recompression index

Table 8. Results of the CPT and other estimated soil properties using the resistance values

Depth (m)	Q_c (Kg/cm^2)	S_r (Kg/cm^2)	Q_{cn} (Kg/cm^2)	F_R	Q_{all} (KN/m^2)	UCS (KN/m^2)	Cu (KN/m^2)	M-number	E_{sq} (KN/m^2)	E_{strip} (KN/m^2)	N_{Cor}	σ_o (KN/m^2)	Q_a Strip	Q_a Square
CPT-1: 706434mE; 798983mN; 264m absl														
0.25	30	97	84	3.23	68.60	12.57	6.28	17	514.50	720	8	4.70	834	1096
0.5	78	267	218	3.42	178.36	32.86	16.43	44	1337.70	1873	20	9.40	2063	2589
0.75	92	241	258	2.62	210.37	38.56	19.28	52	1577.80	2209	23	14.10	2422	3024
1.0	125	323	350	2.58	285.83	52.42	26.21	71	2143.75	3001	31	18.80	3267	4051
CPT-2: 706324mE; 798498mN; 257m absl														
0.25	25	63	70	2.51	57.17	10.41	5.20	14	428.75	600	6	4.97	706	941
0.5	80	230	224	2.88	182.93	33.68	16.84	45	1372.00	1921	20	9.94	2114	2651
0.75	118	264	330	2.24	269.83	49.66	24.83	67	2023.70	2833	30	14.91	3087	3833
CPT-3: 706272mE; 797746mN; 253m absl														
0.25	20	73	56	3.64	45.73	8.27	4.14	11	343.00	480	5	4.88	578	785
0.5	68	226	190	3.33	155.49	28.55	14.27	38	1166.20	1633	17	9.75	1807	2278
0.75	100	295	280	2.95	228.67	41.96	20.98	57	1715.00	2401	25	14.63	2626	3273
1.0	130	326	364	2.51	297.27	54.52	27.26	74	2229.50	3121	33	19.50	3395	4206
CPT-4: 706497mE; 797243mN; 259m absl														
0.25	15	55	42	3.67	34.30	6.13	3.06	8	257	360	4	4.88	449	630
0.5	50	169	140	3.38	114.33	20.83	10.41	28	858	1201	13	9.75	1346	1718
0.75	75	238	210	3.17	171.50	31.24	15.62	42	1286	1801	19	14.63	1986	2496
1.0	85	191	238	2.25	194.37	35.23	17.61	48	1458	2041	21	19.50	2242	2807
1.25	122	256	329	2.10	269.01	48.92	24.46	67	2018	2825	31	24.38	3078	3822
CPT-5: 706774mE; 797261mN; 259m absl														
0.25	22	43	62	1.95	50.31	9.13	4.56	12	377.30	528.22	6	4.88	629	848
0.5	65	151	182	2.32	148.63	27.26	13.63	37	1114.75	1560.65	16	9.75	1730	2185
0.75	80	193	224	2.41	182.93	33.39	16.69	45	1372.00	1920.80	20	14.63	2114	2651
1.0	95	184	266	1.94	217.23	39.49	19.75	54	1629.25	2280.95	24	19.80	2498	3118
1.25	135	271	365	2.01	297.68	54.27	27.13	74	2232.56	3125.59	34	24.75	3399	4212
CPT-6: 706706mE; 796519mN; 254m absl														
0.25	29	83	81	2.87	66.31	12.14	6.07	16	497	696	7	4.63	808	1065
0.5	68	203	190	2.99	155.49	28.58	14.29	38	1166	1633	17	9.25	1807	2278
0.75	82	211	230	2.57	187.51	34.29	17.15	46	1406	1969	21	13.88	2165	2713
1.0	95	221	266	2.33	217.23	39.56	19.78	54	1629	2281	24	18.69	2498	3118
1.25	109	263	273	2.41	222.54	40.27	20.13	55	1669	2337	27	23.36	2558	3190
1.50	142	523	355	3.68	289.92	52.61	26.30	72	2174	3044	36	28.04	3312	4106
CPT-7: 706413mE; 796015mN; 261m absl														
0.25	12	43	34	3.61	27.44	4.85	2.42	7	205.80	288.12	3	4.75	373	537
0.5	29	83	81	2.85	66.31	11.84	5.92	16	497.35	696.29	7	9.49	808	1065
0.75	38	120	106	3.15	86.89	15.40	7.70	21	651.70	912.38	10	14.24	1039	1345
1.0	45	150	126	3.33	102.90	18.02	9.01	25	771.75	1080.45	11	20.35	1218	1563
1.25	69	266	173	3.85	140.88	24.82	12.41	35	1056.56	1479.19	17	25.44	1643	2079
1.50	80	330	200	4.12	163.33	28.72	14.36	40	1225.00	1715	20	30.53	1895	2385
1.75	97	378	170	3.90	138.63	23.77	11.88	34	1039.72	1456	24	35.61	1618	2049

2.0	112	435	197	3.88	160.98	27.64	13.82	40	1207.36	1690.30	28	40.70	1868	2353
CPT-8: 705922mE; 796409mN; 259m absl														
0.25	22	103	62	4.67	50.31	9.13	4.56	12	377	528	6	4.88	629	848
0.5	49	223	137	4.55	112.05	20.40	10.20	28	840	1176	12	9.75	1320	1687
0.75	88	342	246	3.89	201.23	36.82	18.41	50	1509	2113	22	14.63	2319	2900
1.0	123	395	344	3.21	281.26	51.52	25.76	70	2109	2953	31	19.50	3215	3988
CPT-9: 706439mE; 794247mN; 262m absl														
0.25	15	73	42	4.84	34.30	6.12	3.06	8	257	360	4	4.95	449	630
0.5	45	174	126	3.87	102.90	18.64	9.32	25	772	1080	11	10.49	1218	1563
0.75	76	268	213	3.52	173.79	31.60	15.80	43	1303	1825	19	15.74	2012	2527
1.0	98	326	274	3.33	224.09	40.71	20.35	55	1681	2353	25	20.98	2575	3211
1.20	140	323	350	2.31	285.83	51.95	25.98	71	2144	3001	35	26.23	3267	4051

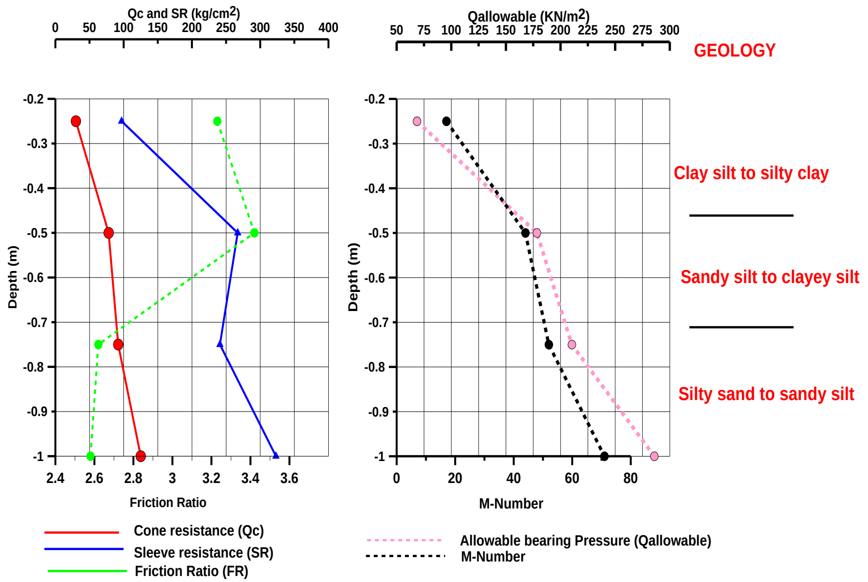

(a)

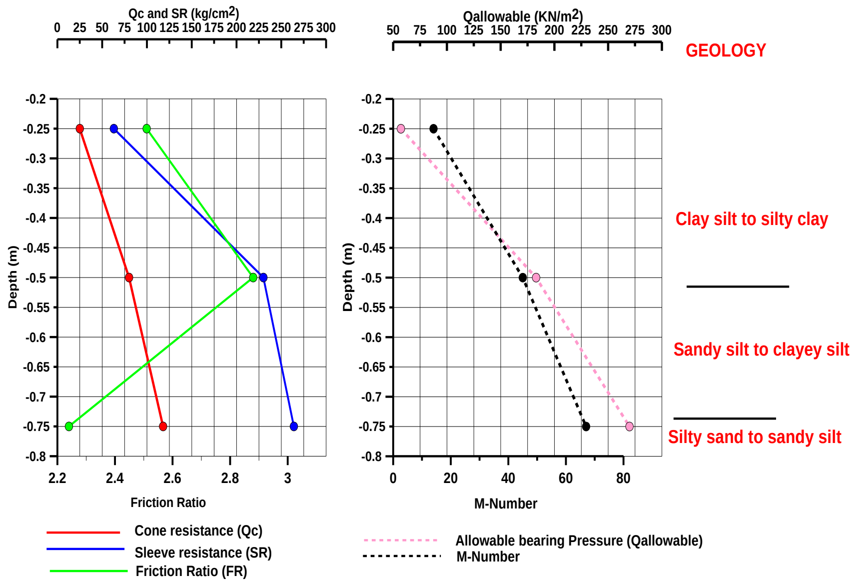

(b)

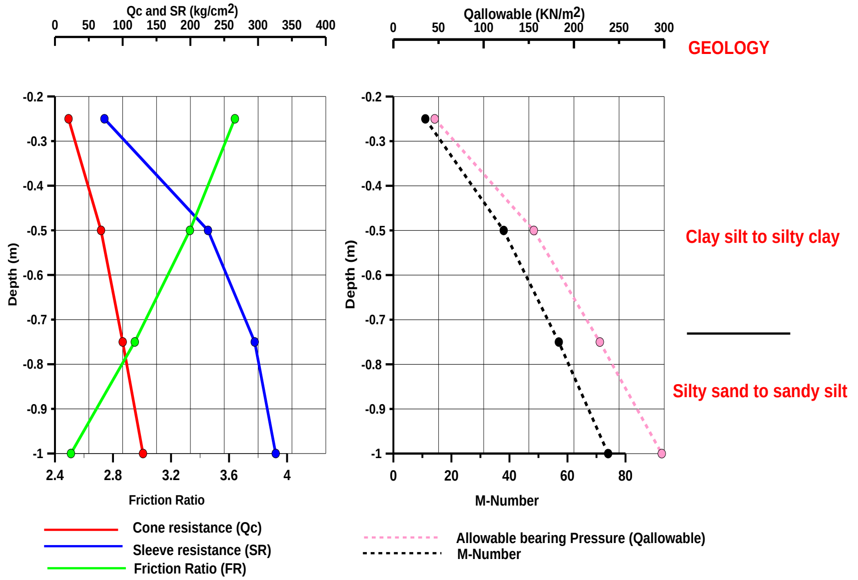
Qc and SR (kg/cm2)
Qallowable (KN/m2)
GEOLOGY
Clay silt to silty clay
Silty sand to sandy silt
Depth (m)
Friction Ratio
M-Number
Cone resistance (Qc)
Sleeve resistance (SR)
Friction Ratio (FR)
Allowable bearing Pressure (Qallowable)
M-Number

(c)

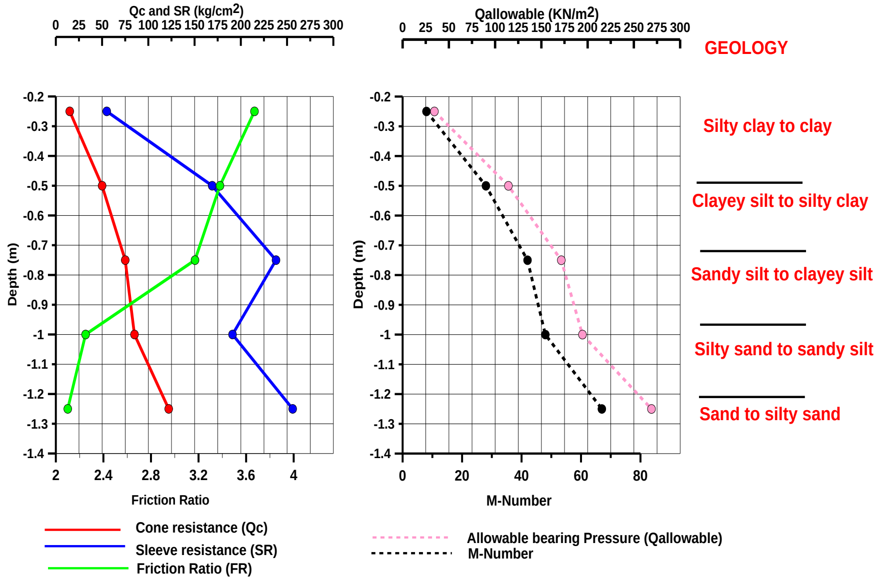
Qc and SR (kg/cm2)
Qallowable (KN/m2)
GEOLOGY
Silty clay to clay
Clayey silt to silty clay
Sandy silt to clayey silt
Silty sand to sandy silt
Sand to silty sand
Depth (m)
Friction Ratio
M-Number
Cone resistance (Qc)
Sleeve resistance (SR)
Friction Ratio (FR)
Allowable bearing Pressure (Qallowable)
M-Number

(d)

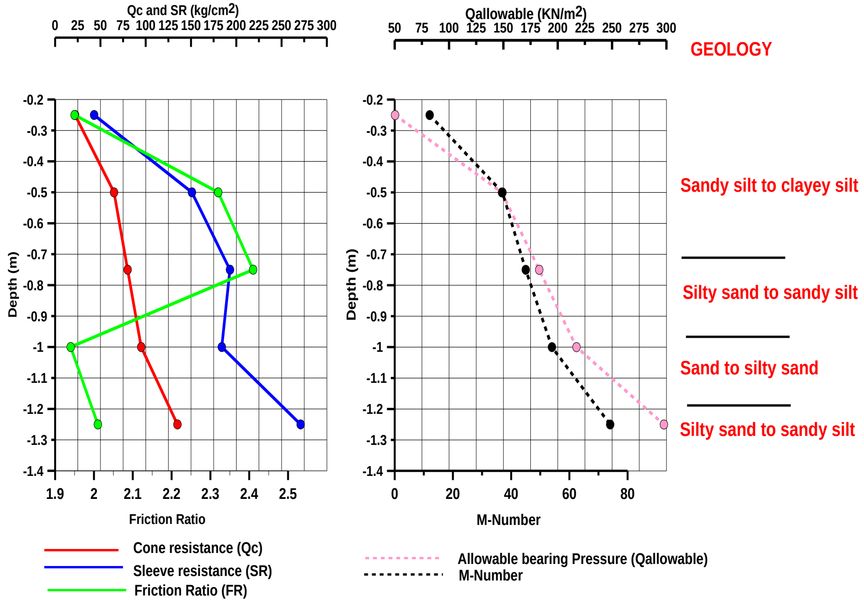
Qc and SR (kg/cm2)
Qallowable (KN/m2)
GEOLOGY
Sandy silt to clayey silt
Silty sand to sandy silt
Sand to silty sand
Silty sand to sandy silt
Depth (m)
Friction Ratio
M-Number
Cone resistance (Qc)
Sleeve resistance (SR)
Friction Ratio (FR)
Allowable bearing Pressure (Qallowable)
M-Number

(e)

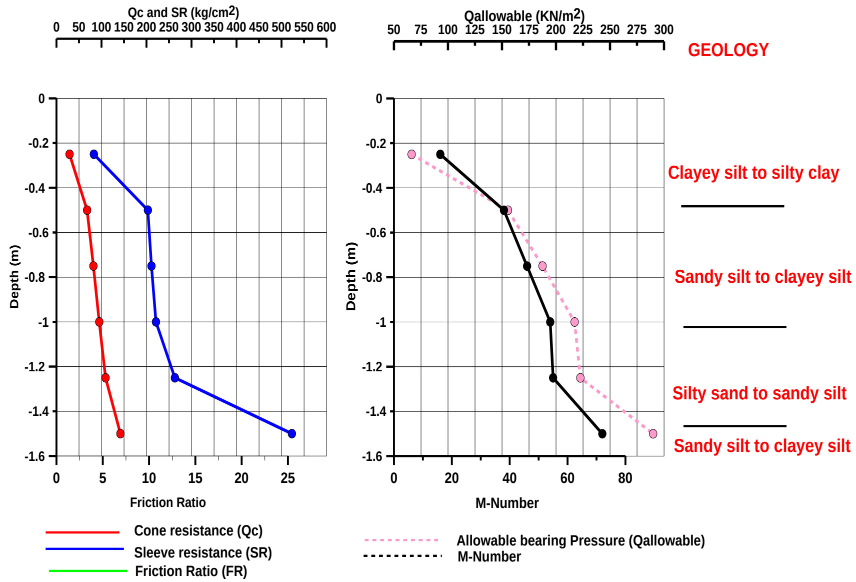
Qc and SR (kg/cm2)
Qallowable (KN/m2)
GEOLOGY
Clayey silt to silty clay
Sandy silt to clayey silt
Silty sand to sandy silt
Sandy silt to clayey silt
Depth (m)
Friction Ratio
M-Number
Cone resistance (Qc)
Sleeve resistance (SR)
Friction Ratio (FR)
Allowable bearing Pressure (Qallowable)
M-Number

(f)

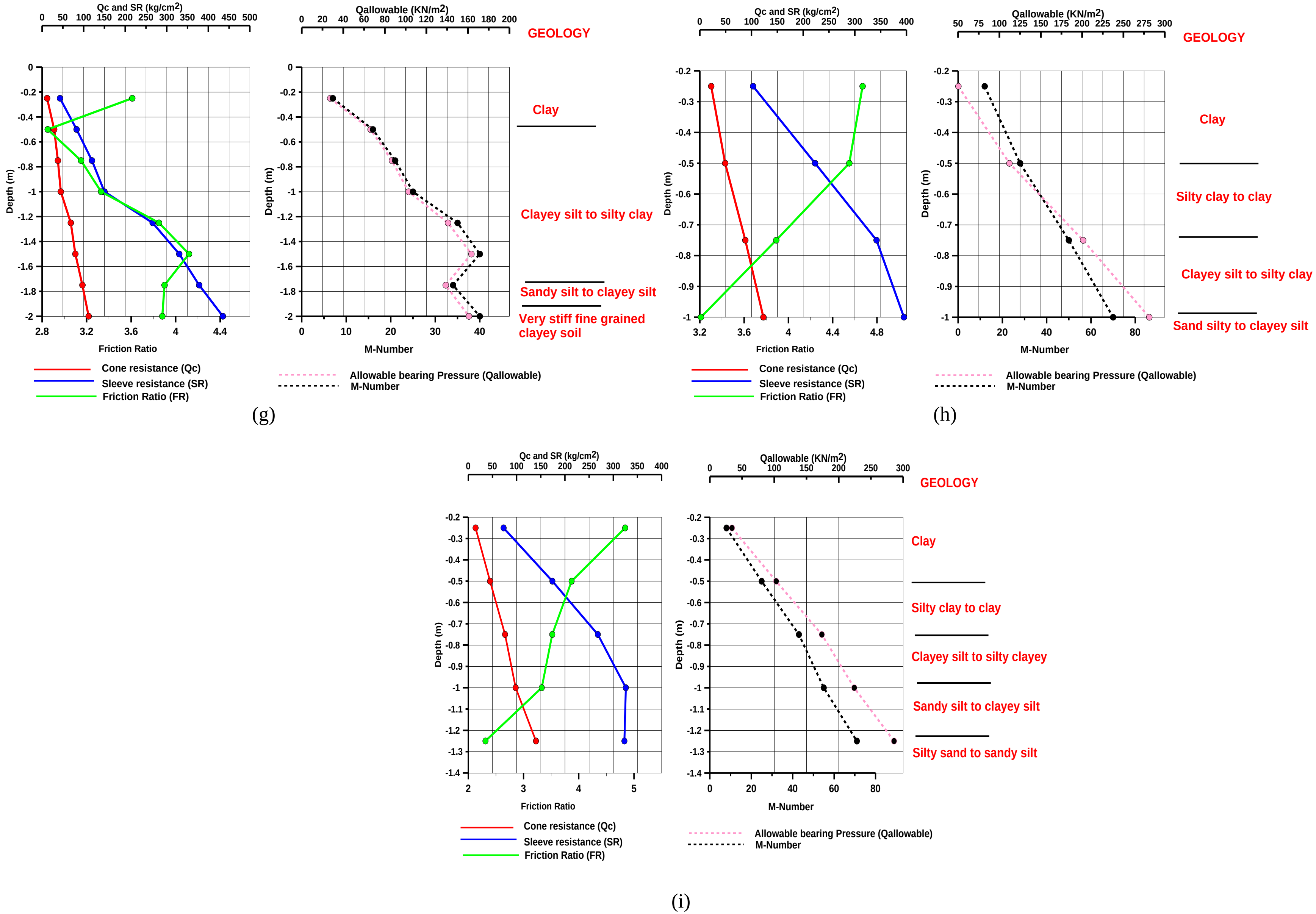

Fig. 9. The Interpreted CPT Data obtained from Study Area at the nine locations respectively, showing the plots of cone resistance, sleeve resistance, friction ratio, allowable bearing pressure, and M-Number with respect to depth.

Geotechnical Parameters modeling and correlations

The obtained graphs for the parameters correlated are shown in Figure 10. The obtained MDD/PI was correlated with soaked CBR determined from the laboratory and gives weak positive correlation (R^2) of 0.0043 and linear regression model (equation 11):

CBR (soaked) = 0.0035x + 6.5283 (Eq.11)

In this relationship, x = MDD/PI

The LL was plotted against coefficient of consolidation. This gives a regression model of equation 12, with weakly positive correlations (R^2) of 0.0608.

Coefficient of consolidation = 9E-05x + 0.0071 (Eq. 12)
In these relationships, x = LL

The relationship between PI and undrained shear strength/effective overburden, is shown by the regression model in equation 13, with R^2 of 0.2706.

$\frac{undrained\ shear\ strength}{effective\ overburden}$ = 0.1551x + 1.5577 (Eq.13)
Where x is PI.

The correlation between dry density and angle of shearing gives equation 14, with correlation coefficient of 0.0058.

Angle of shearing = -0.2531x + 22.469 (Eq. 14)
Where x is dry density

The plot of PI and angle of shearing, gives correlation coefficient of 0.0117, and the model is presented in equation 15.

Angle of shearing = -0.1821x + 21.09 (Eq. 15)
Where x is PI.

The relationship between suitability index and soaked CBR, gives a weak positive correlation of 0.3644, and the regression model shown in equation 16.

CBR (soaked) = -7.6065x + 16.162 (Eq.16)
Where x is suitability index.

In addition, the obtained clay content was correlated with PI and gives weak positive correlation (R^2) of 0.1355 and linear regression model (equation 17).

PI = 0.0727x + 16.949 (Eq.17)

Where x is clay content.

Implication for varying Civil Engineering Construction

Pavement and Airfield

Pavement construction is generally shallow given that pavements are normally founded relatively close to the surface. A pavement investigation will often include surface exploration including a walkover survey to observe existing conditions and performance of existing pavements and subsurface exploration of a site using drilling or other excavation methods (Brown, 1996). Subsurface exploration usually involves soil sampling, sampling of existing pavement materials for potential re-use or stabilization in-situ test and laboratory tests of the soil and pavement materials samples retrieved (Weltman and Head, 1983). The engineering properties of soil desired for foundation under highway and airfield should have adequate strength, good compaction, adequate drainage, and acceptable compression and expansion properties. The design of flexible pavement is normally based on Group Index method or California Bearing Ratio method (George and Uddin, 2000; Wright, 1986). The drainage characteristics of the soil is poor with soaked CBR generally less than 10. The AASHTO classification of the soils for subgrade varied from A-2-4 (IL-03), A-7-6 and A-6-5 (IL-17). However, the A7-6 are the most dominant (Table 9) and USCS of the soils is CL and CH. This type of soils are generally poor in highway subgrade construction. From the result of the study, the GI ranged from 1-11 (avg. 6) corresponding to fair subgrade for highway construction, with expected recommended minimum -thickness of 241 – 513 mm (avg. 394.7 mm) obtained from design curves (Table 9). The average soaked CBR of the soils is 7% which fell below 10% recommended standard for subgrade, base or subbase. Thus, the soil is unsuitable for subgrade, base and sub-base courses (FHWA, 2006). Consequently, an inexpensive/economic mechanical stabilization or soil gradation and compaction will help in improving the bearing capacity and drainage characteristics of the soils for pavement construction.

Building Foundation

The average allowable bearing capacity of the soil for square and round foundations in Table 9 varied from 234 – 297 KN/m^2 (avg. 268 KN/m^2) and 232 – 298 KN/m^2 (avg. 268 KN/m^2). The estimated immediate/elastic settlement ranged from 6.76 – 7.66 mm (avg. 7.13 mm); and consolidation settlement varied between 0.75 – 11.62 mm (avg. 9.65 mm). The total settlement obtained is in between 17.69 – 18.88 mm (avg. 18.28 mm) for structural pressure of 100 KN/m^2. This form of settlement is peculiar to fine grained soils such as clay, silt (plastic silt). From the CPT result, the average allowable pressure was estimated to be 162.56 KN/m^2 for average depth of 1.5 m. These bearing pressures are fair and would only be suitable for light/medium weight structures, with adequate factor of safety. The bearing pressures (using Hatanaka & Uchida, 1996; Mayne, 2001; Schmertmann, 1975; and Meyerhof, 1956 equations) gave model bearing capacity with respect to foundation width as shown in Figure 11. The deformation criterion was calculated using Burland and Burbridge (1984) equation. The applied factor of safety is 3.0, for maximum allowable settlement of 25.0 mm However proper soil improvement methods must be adopted (since clay/plastic silt tends to undergo volume change when desiccated), to ensure that the settlement is reduced in relation to the bearing pressure,

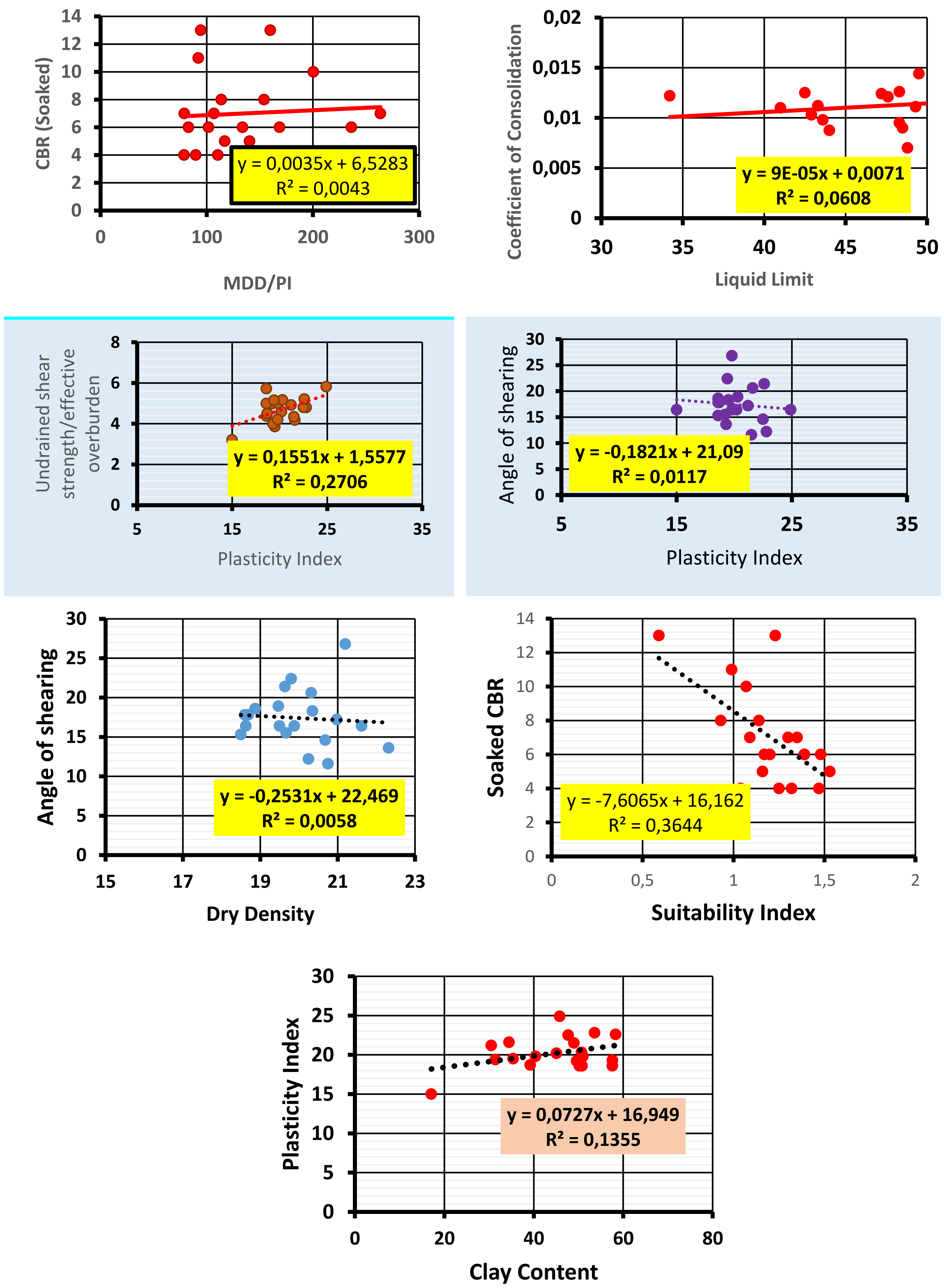

Fig. 10. Geotechnical parameters correlation for some of the engineering properties of the soils

although the soil are characterized by LL in the range of 30 – 60 %, therefore according to Table 10 the soils will undergo medium swelling potential, which corroborates the low compression index (avg. 0.0443) and coefficient of volume compressibility (avg. 0.2041 m^2/KN) recorded for the soils. Summarily the estimated settlement is within the standard 25 mm for building foundations pressure of 100 KN/m^2.

Embankment

The engineering properties of soils used for embankment, such as their shear strength and compressibility are influenced by the amount of compaction they have undergone (Bell, 2007). Thus, for satisfactory performance of an embankment material, the soils should have high stability and strength and well graded; coarse grained (such as sand, gravel) is usually preferable to fine soil. The suitability index of the soils ranged from 0.59 – 1.53 (avg. 1.21). The USCS classification of the soil is CL/CH which depicts soils of poor stability for civil engineering construction; although it will be for impervious core for flood control structures (Attewell and Farmer, 1988).

The suitability index of the soil suggests a fair/expanding not collapsible construction material, as shown also in Figure 12 having low-medium swelling potential. The compaction characteristics of the soil is fair. CL/CH soils have low to medium compressibility and expansion, while the drainage characteristics is poor to practically impervious. Thus, since the soils have high MDD at moderate OMC (avg. 1980 kg/m^3; 14.8 %) greater than 1500 kg/m^3, they are ordinarily considered suitable (Upadhyay, 2015; Carter and Bentley, 1991).

The American Association of State Highway and Transportation Official (AASHTO, 2006) classification of the soils are predominantly A-7-6, and are typical of plastic clay having a high percentage passing 0.075 mm and usually characterized with high volumetric change between wet and dry states. A-7-6 materials have high plasticity indices in relation to the liquid limits and are subject to extremely high volume change. Therefore, the soils with A-7-6/A-6 fines can be placed at the bottom of embankment and to remain in the top 0.5 m below subgrade in highway construction.

Therefore, comparing the important soils parameters such as plasticity, compressibility, strength (shear), workability, and compaction characteristics, the soils are rated according their utility for dams, canals, foundations, and highway. The relative score given to the soil is in the order of desirability from 1 to 14 i.e. high to low relevance, respectively. The findings from this study also confirmed some earlier suggestions to the effect that the coarser the material, the greater generally is its strength and the finer the material, the worse are its engineering properties. Thus, from the Table 11, the soil are generally below average or poor.

Rock units

The rocks mapped in the study area are granite, gneiss, migmatite (Figure 13). These rocks are usually characterized by high crushing strength and thus can be trusted in most construction works, especially as building foundation and road stones (Winkler, 1973; Smith, 1999; Prentice, 1990). Igneous rocks, such as fresh granite, are impervious, hard and strong and form very strong foundation for most civil engineering projects such as dams, reservoirs; because of their low porosity (Bell, 2007; Latham, 1998; McNally, 1998). The granitic rocks are rich in quartz, feldspar, and accessory mica (muscovite, biotite), amphiboles (hornblende), augite, hyperstene, magnetic, apatite, garnet, and tourmaline. Their texture ranged from medium to coarse grained, while some are porphyritic (Figure 13a). The gneisses are megascopically crystalline foliated metamorphic rocks. They are characterized with mineral segregation into layers or bands of contrasting colour, texture and composition. Its common minerals are mica, feldspar, hornblende and quartz. The texture is medium to coarse with poor mineral arrangement. The gneisses show bands of micaceous minerals alternating with bands of equidimensional minerals like feldspar, quartz (Figure 13b). The migmatite are mixed rocks that consist of intimately associated members of igneous rock (granitic rock) and metamorphic (gneisses) groups. They are widespread in the study area.

The compressive strength of a rock depends on a number of factors such as mode of formation, composition, texture, structure, moisture content, and extent of weathering. According to Hunt (2005) igneous rock have been crystalline in character, compact, and interlocking in texture and uniform in structure, and possess very high compressive/shear strength, modulus of elasticity. However, for metamorphic rocks the foliation, schistocity, and cleavage greatly affect their compressive strength in magnitude and direction. Table 11 showed that the residual soils of most granites, gneisses and migmatite are low activity clays and granular soil, which is in agreement with earlier results, while Table 12 showed the expected properties of rocks observed in the study area.

Table 10. Estimating Probable Swelling Pressure (After Carter and Bentley, 1991)

Laboratory and Field data					
Percent passing 0.075mm	Liquid limit (%)	Standard penetration resistance, blows/300 mm	Probable expansion percent total volume change	Swelling pressure (KN/m^2)	Degree of expansion
>35	>60	>30	>10	>1000	Very High
60-95	40-60	20-30	3-10	250-1000	High
30-60	30-40	10-20	1-5	150-250	Medium
<30	<30	<10	<1	<50	Low

Table 9. The Highway and Foundation Characteristics of the soil with expected settlements

Sample No.	Subgrade Rating		GI Class	Rec Thickness (mm)	Suitability Index	Bearing Capacity (KN/m^2) Square Footing		Bearing Capacity (KN/m^2) Round Footing		Settlement (mm)		
	USCS	AASHTO Class				Q_T	Q_A	Q_T	Q_A	Elastic	Consol	Total
IL-1	Poor to Fair	Good	Poor	368	0.93	830	276	893	298	7.66	1.1227	18.59
IL-2	Poor to Fair	Fair	Poor	508	1.32	829	277	846	282	7.21	1.2001	18.41
IL-3	Good	Excellent	Good	254	0.59	713	238	732	244	6.76	0.751	17.82
IL-4	Poor to Fair	Excellent	Poor	381	1.30	839	280	857	286	6.89	11.07	17.96
IL-5	Poor to Fair	Excellent	Poor	419	1.17	767	256	759	253	6.91	11.08	17.99
IL-6	Poor to Fair	Good	Poor	419	1.48	873	291	865	289	6.96	11.2	18.16
IL-7	Poor to Fair	Fair	Poor	513	1.04	891	297	883	284	7.03	11.05	18.08
IL-8	Poor to Fair	Good	Poor	513	1.25	827	276	819	273	6.9	11.11	18.01
IL-9	Poor to Fair	Excellent	Poor	279	1.07	777	259	770	257	7.28	11.56	18.84
IL-10	Poor to Fair	Fair	Poor	419	1.39	856	285	849	283	6.79	10.9	17.69
IL-11	Poor to Fair	Fair	Poor	419	1.20	846	282	839	280	7.2	10.91	18.11
IL-12	Poor to Fair	Fair	Poor	368	1.14	764	255	757	252	7.24	11	18.24
IL-13	Poor to Fair	Fair	Poor	445	1.53	736	245	729	243	7.12	10.95	18.07
IL-14	Poor to Fair	Good	Poor	455	1.35	813	271	805	269	6.9	11.02	17.92
IL-15	Poor to Fair	Fair	Poor	381	1.47	775	258	768	256	7.26	11.62	18.88
IL-16	Poor to Fair	Fair	Poor	381	1.09	702	234	695	232	7.42	11.3	18.72
IL-17	Poor to Fair	Poor	Poor	267	0.99	786	262	779	260	7.25	11.35	18.6
IL-18	Poor to Fair	Fair	Poor	445	1.16	836	279	829	276	7.41	11.25	18.66
IL-19	Poor to Fair	Poor	Poor	241	1.23	778	259	771	257	7.29	11.2	18.49
IL-20	Poor to Fair	Fair	Poor	419	1.39	862	287	855	285	7.07	11.26	18.33

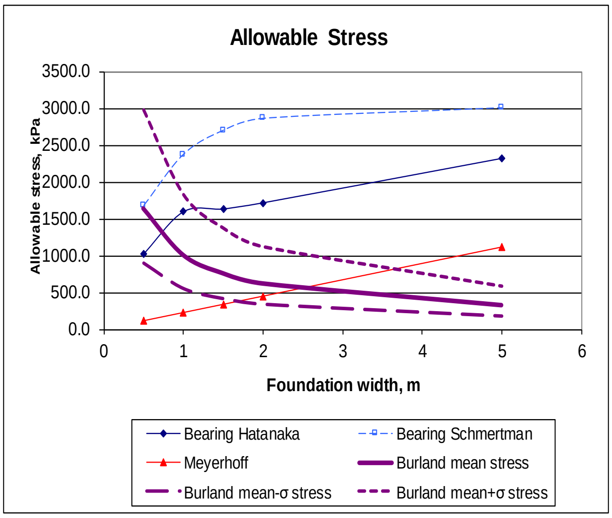

(a) CPT 1

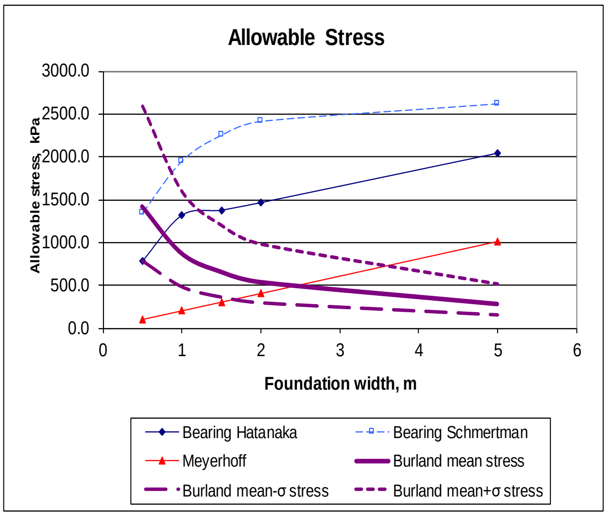

(b) CPT 2

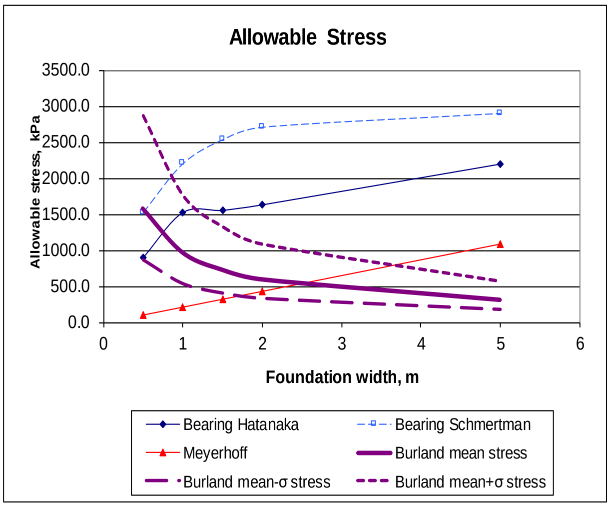

(c) CPT 3

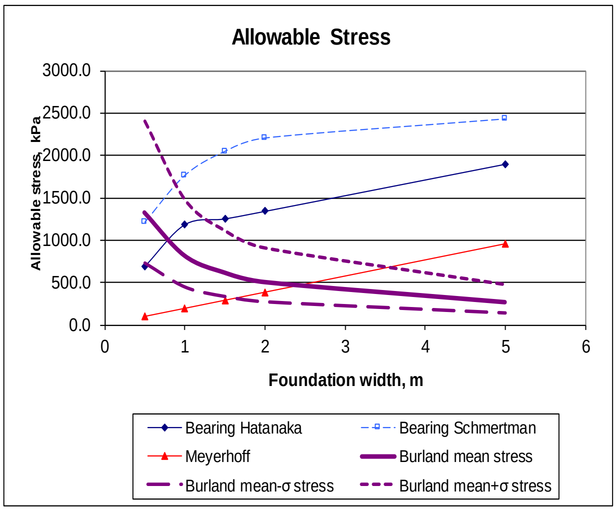

(d) CPT 4

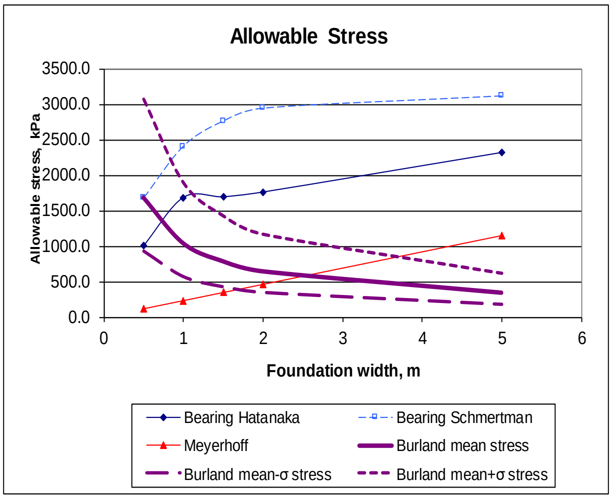

(e) CPT 5

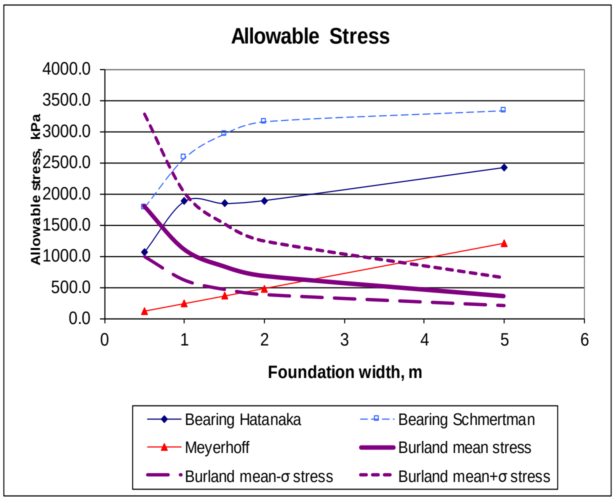

(f) CPT 6

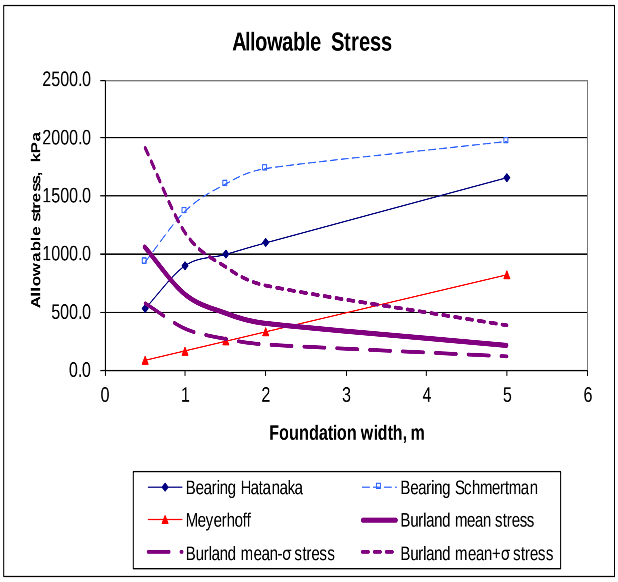

(g) CPT 7

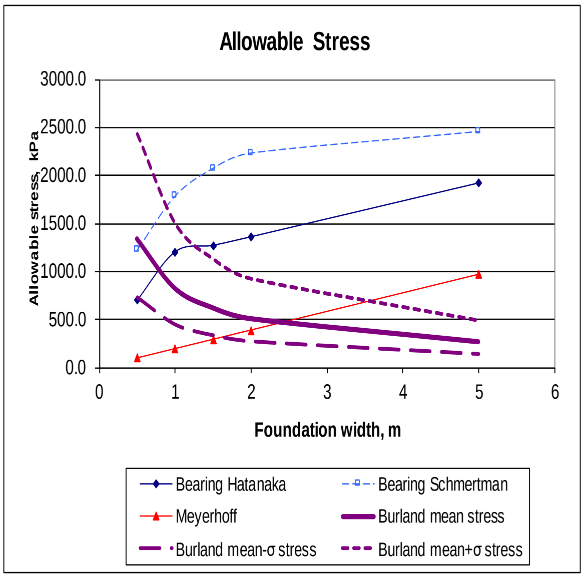

(h) CPT 8

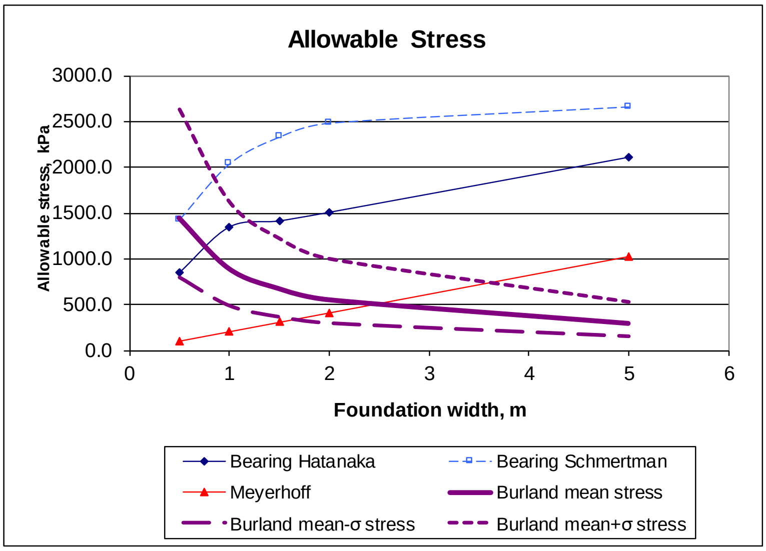

(i) CPT 9

Fig. 11. Model Graph of the bearing pressure and stresses for various footing width using CPT 1 to 9 data for maximum allowable settlement of 25 mm

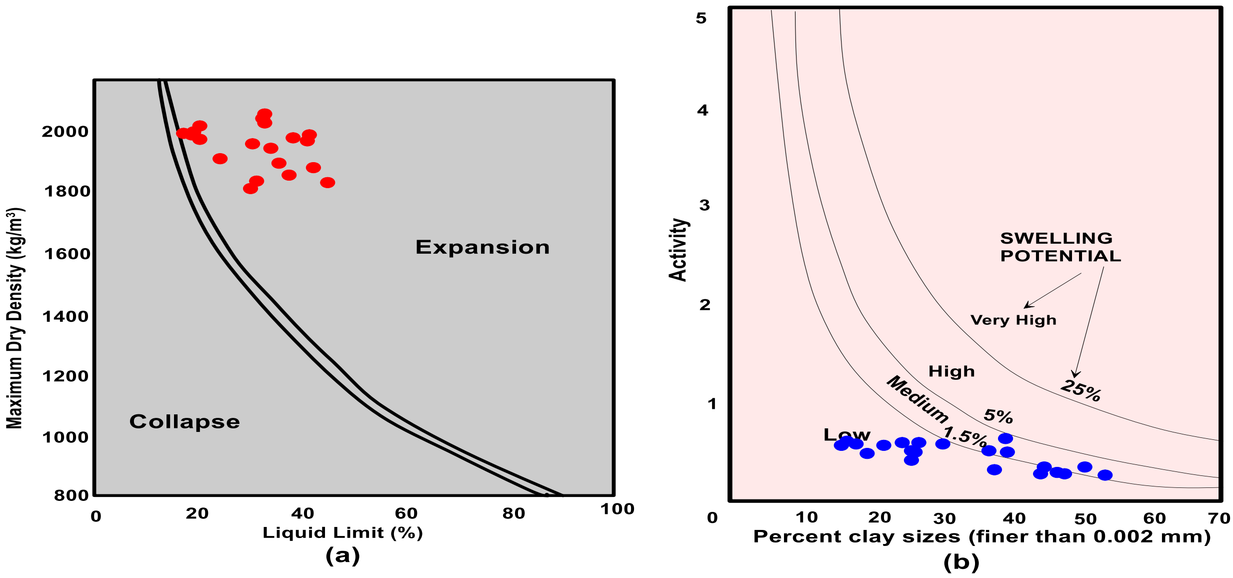

Fig. 12. Workability and swelling potential of the soils Classification chart for swelling potential (After Carter and Bentley, 1991; Holtz and Kovacs, 1981)

Table 10. Summary of desirability potential of the soil for various engineering uses

Various uses	Properties	Characteristics/relative suitability
Important Engineering parameter/property	Permeability when compacted	Semi impervious- impervious
	Shear strength when compacted saturated	Fair
	Compressibility when compacted saturated	Fair
	Workability as construction material	Fair
Earth fill dams	Rolled Earth fill dams (homogeneous embankment)	S: 6
	Rolled Earth fill dams (core/shell)	S: 5
Canal	Canal sections (erosion resistance)	S: 10
	Canal sections (compacted earth lining)	S: 4, where erosion is critical 4
Foundation	Foundations (where seepage is important)	S: 7
	Foundations (where seepage not important)	S: 10
Roadway	Roadway fills	S: 10
	Roadway surfacing	S:10

Table 11. Classification of residual soils by its primary origin (Hunt, 2005)

Primary occurrence	Secondary occurence	Typical residual soils
Granite	Saprolite	Low activity clays and granular soils
Diorite		
Gabroo	Saprolite	High activity clays
Basalt		
Dolerite		
Gneiss	Saprolite	Low activity clays and granular soils
Schist		
Phyllite		Very soft rock
Sandstone		Thin cover depends on impurities. Older sandstones would have thicker cover
Shales	Red	Thin clayey cover
	Black, marine	Friable and weak mass high activity clays
Carbonates	Pure	No soil, rock dissolves
	Impure	Low to high activity clays

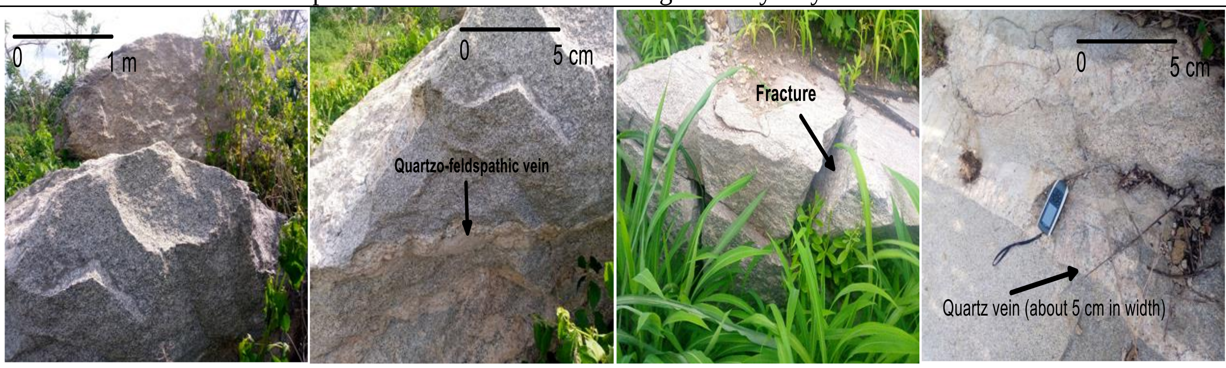

(a) Surface exposures and outcrops of granite at different locations having being subjected to intense weathering, some occuring as boulders with noticeable fractures/fissures. In addition feldspathic and quartzo-feldspathic intrusion are observed

(b) Surface exposures and outcrops of migmatites and granite gneiss at different locations having being subjected to intense weathering, with noticeable fractures/fissures. In addition feldspathic and quartzo-feldspathic intrusion are also observed

Fig. 13. Surface exposure/outcrops of (a) granite (b) gneiss, and migmatite observed in the study area

Table 12. General engineering properties of common rocks (Hunt, 2005)

Rock origin	Type	Characteristics	Permeability	: Deformability	Strength
Igneous coarse to medium grained – very slow to slow cooling	Granite, granodiorite, diorite, peridiorite	Welded interlocking grains, very little pore space	Essentially impermeable	Very low	Very high
Igneous fine grained – rapid cooling	Rhyolite, trachyte, quartz, dacite, andesite, basalt	Similar to above or can contain voids	With voids can be highly permeable	Very low to low	Very high to high
Igneous glassy – very rapid chilling	Pumice, scoria, vesicular basalt	Very high void ratio	Very high	Relatively low	Relatively low
Sedimentary – arenaceous clastic	Sandstones	Voids cement filled.	Low	Low	High
		Partial filling of voids by cement coatings	Very high	Moderate to high	Moderate to low
Sedimentary – argillaceous clastic	Shales	Depends on degree of lithification	Impermeable	High to low, can be highly expansive	Low to high
Sedimentary – arenaceous clastic chemically formed	Limestone	Pure varieties normally develop caverns	High through caverns	Low except for cavern arch	High except for cavern arch
Metamorphic	Gneiss	Weakly foliated	Essentially impermeable	Low	High
		Strongly foliated	Very low	Moderate normal to foliations. Low parallel to foliations	High - normal to foliations. Low parallel to foliations
Metamorphic	Schist	Strongly foliated	Low	As for gneiss	
Metamorphic	Phyllite	Highly foliated	Low	Weaker than gneiss	
Metamorphic	Quartzite	Strongly welded grains	Impermeable	Very low	Very high
Metamorphic	Marble	Strongly welded	Impermeable	Very low	Very high

Table 13. Estimate of allowable bearing capacity in rock (Hunt, 2005)

	Presumed allowable bearing capacity (kPa)			
	XW	DW	SW	FR
Igneous				
Tuff	500	1,000	3,000	5,000
Rhyolite, Andesite, Basalt	800	2,000	4,000	8,000
Granite, Diorite	1,000	3,000	7,000	10,000
Metamorphic				
Schist, Phyllite, Slate	400	1,000	2,500	4,000
Gneiss, Migmatite	800	2,500	5,000	8,000
Marble, Hornfels, Quartzite	1,200	4,000	8,000	12,000
Sedimentary				
Shale, Mudstone, Siltstone	400	800	1,500	3,000
Limestone, Coral	600	1,000	2,000	4,000
Sandstone, Greywacke, Argillite	800	1,500	3,000	6,000
Conglomerate, Breccia	1,200	2,000	4,000	8,000

The rocks are expected to have very high strength, low deformability; and presumable bearing capacity of 8, 000 – 10, 000 KPa (Table 13) especially when fresh (FR), and can be in between 5000 – 7000 KPa when partly or slightly weathered (SW). Falowo (2019) conducted geotechnical analysis of some rocks (porphyritic granite, fine grained granite, migmatite, granite gneiss, quartz schist, granodiorite, charnockite, and quartzite) within the same geological province, for aggregate impact value, aggregate crushed value, point load strength test, specific gravity, water absorption and unconfined compression test, and direct shear strength using BS, ASTM D-2216 and ISRM procedures. These rocks are supposed to be contemporaneous with those in the study area, as they both displaced the same structural features in magnitude and direction. The Aggregate Impact Value (AIV) ranged 11.2 (granite gneiss) to 15.2 (porphyritic granite), Aggregate crushed value (ACV) 19.7 – 24.2, and unconfined compressive strength (UCS) varied from 121.1 MPa (porphyritic granite) – 143.1 MPa (granite). Higher UCS values above 150 MPa were recorded for charnockite, grandiorite, quart schist, and quartzite. All the rocks are characterized with AIV, ACV, and UCS, with point load strength index (PLSI) ranged between 7.40 MPa – 8.82 (granite gneiss), and shear strength of 60.5 MPa (porphyritic granite) to 71.6 MPa (granite). Therefore, the rocks have high value as foundation constructions, aggregate in pavement, building stone, and armourstones (Smith and Collis, 2001; Archana and Kumar, 2016).

Conclusion

This study has demonstrated the usefulness of geo-informatics in the area of establishment of subsoil engineering database, as baseline information for civil engineering design, construction, and management in Ile-Oluji area of Ondo State, Southwestern Nigeria. The findings from the study showed the soil to be dominantly clay of low to high plasticity and compressibility with average % fines of 47.5. The depth to groundwater ranged from 2.1 m (in well) – 21.8 m (in borehole). The average depth to basement rock is 22.4 m indicating a moderate to deep weathering profile, able to support burial of engineering utilities. The soil are generally inactive type with predominant illite clay mineralogy group, with activity of 0.48. The soil showed good strength/shear characteristics of 186.8 KN/m2 (USC), 17.4° (angle of friction), 48.4 KN/m^2 (cohesion) with unit weight of 19.99 KN/m^3.

Consequently, the soil is unsuitable for subgrade, base and sub-base courses with CBR less than 7% and GI of 6 (avg.), thus it's expected to support minimum highway thickness of 241 – 513 mm (avg. 395 mm) obtained from design curves. Thus an inexpensive/economic mechanical stabilization or soil gradation and compaction will help in improving the bearing capacity and drainage characteristics. The average allowable bearing capacity of the soil for square and round foundations are 268.4 KN/m^2 and 267.95 KN/m^2 respectively, with average total settlement of 18.3 mm for structural pressure of 100 KN/m^2. For embankment, the suitability index (1.21) of the soil suggests a fair/expanding not collapsible construction material, as shown since the soils have high MDD at moderately high OMC (avg. 1980 kg/m^3; 14.8 %) greater than 1500 kg/m^3, they are ordinarily considered suitable.

Rocks of igneous and metamorphic rock are widespread in the study area including granite, gneiss, and migmatite, some are outcropped while some are deep seated within the subsurface. However, it is expected for the rock to have very high compressive/shear strength, modulus of elasticity, high crushing strength, low deformability; and presumable bearing capacity of 8, 000 – 10, 000 KPa especially when fresh (FR), and can be in between 5000 – 7000 KPa when partly or slightly weathered (SW) and thus can be trusted in most construction works, especially as foundation and road stones, because of their presumable high values for aggregate impact value, aggregate crushed value, point load strength test, unconfined compression test, and direct shear strength for the rock in northern area of the same geological province which are contemporaneous in history. Therefore the rocks have high value as foundation constructions, aggregate in pavement, building stone, and armourstones.

Acknowledgements

The author is grateful to TETFund, Nigeria (under the Institution Based Research) Nigeria. Special appreciation to all students of Civil Engineering Technology Department for the assistance rendered during data acquisition.

References

AASHTO (2006). Standard Specifications for Transportation Materials and Methods of Sampling and Testing, Parts I and II, American Association of State Highway and Transportation Officials, Washington, D.C.

Adejumo, S.A., Oyerinde, A.O., Akeem, M.O. (2015). Integrated geophysical and geotechnical subsoil evaluation for pre-foundation study of proposed site of vocational skill and entrepreneurship center at the polytechnic, Ibadan, SW, Nigeria. *Int J Sci Eng Res* 6: 910-917.

Adewuyi, O.I., Philips, O.F. (2018). Integrated Geophysical and Geotechnical Methods for Pre-Foundation Investigations. *J Geol Geophys* 8: 453. doi:10.4172/2381-8719.1000453

Alabi, A.A., Adewale, A.O., Coker, J.O., Ogunkoya, O.A. (2017). Site Characterization for Construction Purposes at FUNAAB using Geophysical and Geotechnical Methods, *RMZ – M&G*, Vol. 65, pp. 089–102. DOI: 10.2478/rmzmag-2018-0007

Alaminiokuma, G.I., Chaanda, M.S. (2020). Geophysical Investigation of Structural Failures Using Electrical Resistivity Tomography: A Case Study of Buildings in FUPRE, Nigeria. Journal of Earth Sciences and Geotechnical Engineering, Vol.10, No.5, 2020, 15-33.

Archana, P.M., Padma, K.R. (2016). Engineering and Geological Evaluation of Rock Materials as Aggregate for Pavement Construction. *International Advanced Research Journal in Science, Engineering and Technology*, Vol. 3, Special Issue 3, August 2016. DOI 10.17148/IARJSET

Arora, K.R. (2008). Soil mechanics and foundation engineering (Geotechnical Engineering). Standard Publishers Distributors, Delhi.

ASTM (2006). Annual Book of ASTM Standards – Sections 4.02, 4.08, 4.09 and 4.13. ASTM International, West Conshohocken, PA.

Attewell, P.B., Farmer, I.W. (1988). Principles of engineering geology Principles of Engineering Geology John Wiley & Sons, Inc, New York, 1045pp. ISBN-13: 978-94-009-5709-1 DOl: 101007/978-94-009-5707-7

Bawallah, M.A., Ilugbo, S.O., Ozegin, K.O., Adebo B.A., Aigbedion, I., Salako, K.A. (2021). Electrical Resistivity and Geotechnical Attributes and the Dynamics of Foundation Vulnerability. Indonesian Journal of Earth Sciences, Vol. 1, No. 2 (2021): 84-97. DOI: 10.52562/injoes.v1i2.253

Bell, F.G. (2007). Engineering Geology Second Edition, Elsevier Limited

Bell, F.G. (2004). Engineering Geology and Construction Spon Press, London

Brassington, R. (1988). Field Hydrogeology. Wiley, Chichester.

Brown, S.F. (1996). Soil mechanics in pavement engineering. *Geotechnique*, 46, 383–426.

BS 1377 (1990). Methods of Tests for Soils for Civil Engineering Purpose, British Standard Institution HMSO London.

Burland, J.B., Burbidge, M.C. (1984). Settlement of foundations on sand and gravel, *Proceedings of the Institution of Civil Engineers,* Part 1, 1985, 78, Dec., 1325-1381.

Carter, M., Bentley, S.P. (1991). Correlations of soil properties, Pentech Press Publishers, London, 129pp

Carter, M., Symons, M.W. (1989). Site Investigations and Foundations Explained. Pentech Press, London.

Cetin, K.O., Ozan, C. (2009). CPT-based probabilistic soil characterization and classification. *J Geotech Geoenviron Eng* 135(1):84–107. doi:10.1061/(ASCE)1090-0241(2009)135:1(84).

Coker, J.O. (2015). Integration of Geophysical and Geotechnical Methods to Site Characterization for Construction Work at the School of Management Area, Lagos State Polytechnic, Ikorodu, Lagos, Nigeria. *International Journal of Energy Science and Engineering*, 1(2), 40-48.

Craig, C. (Ed.). (1996). Advances in Site Investigation Practice. Thomas Telford Press, London.

Das, B.M. (2015). Principles of foundation engineering. Cengage learning, Boston

Eebo, F.O., Samuel, A.B., Olayanju, G.M. (2022). Geophysical and Geotechnical Investigations for Subsoil Competence at a Proposed Hostel Site at Oba Nla, Akure Southwestern Nigeria. Journal of Engineering Research and Sciences, 1(2): 41-49, 2022. DOI: https://doi.org/TBA

Falowo, O.O., Dahunsi, S.D. (2020). Geoengineering Assessment of Subgrade Highway Structural Material along Ijebu Owo – Ipele Pavement Southwestern Nigeria. *International Advanced Research Journal in Science, Engineering and Technology* (IARJSET) Vol 7, Issue 4, 10pp. DOI 1017148/IARJSET20207401

Falowo, O.O., Olabisi, W. (2020). Engineering Geological and Geotechnical Site Characterization for Economic Design of Structures and *Earthwork Journal of Research and Innovation for Sustainable Society*, 2(2), pp43-60. Doi: 1033727/jriss202027:43-60

Falowo, O.O., Ojo, O.O., Daramola, A.S. (2015). The use of magnetic survey in engineering site characterization. *International Journal of Innovative research and development*, Vol., 4(13): pp. 74-85.

Falowo, O.O. (2019). Engineering properties of some basement rocks of Nigeria as Aggregate in Civil Engineering Pavement Construction. *Asian Review of Environmental and Earth Sciences*, Vol. 6, No. 1, 28-37. DOI: 10.20448/journal.506.2019.61.28.37

Faseki, O.E., Olatinpo, O.A., Taiwo, O.B. (2016). Ground Investigation of an Engineering Site at Point Road, Apapa, Lagos, Nigeria. *Journal of Engineering and Energy Research*, 6(1), pp. 1–20.

Federal Meteorological Survey (1982). Atlas of the Federal Republic of Nigeria, 2nd Edition, Federal Surveys, 160pp.

Federal Ministry of Works and Housing. (1997). General Specifications for Roads and Bridges. Volume II.145-284. Federal Highway Department: Lagos, Nigeria.

FHWA NHI-05-037. (2006). Geotechnical aspects of pavement. U.S. Department of Transportation Federal Highway Administration, 4-17.

George, K.P., Uddin, W. (2000). Subgrade characterization for highway pavement design, final report. Jackson, MS: Mississippi Department of Transportation.

Hatanaka, M., Uchida, A. (1996). Empirical correlation between penetration resistance and effective friction of sandy soil. Soils & Foundations, Vol. 36 (4), 1-9, Japanese Geotechnical Society.

Hawkins, A.B. (Ed.). (1986). Site Investigation Practice: Assessing BS 5930. Engineering Geology Special Publication No. 2, Geological Society, London.

Holtz, R.D., Kovacs, W.D. (1981). An Introduction to geotechnical engineering, Prentice Hall.

Hunt, R.E. (2005). Geotechnical engineering investigation handbook, second edition, Taylor and Francis.

Iloeje, P.N. (1981). A new geography of Nigeria. Longman Nigeria Limited, Lagos.

Kamtchueng, B.T., Onana, V.L., Fantong, W.Y., Ueda, A., Ntouala, R.F.D., Wongolo, M.H.D., Ndongo, G.B., Ze, A.N., Kamgang, V.K.B., Ondoa, J.M. (2015). Geotechnical, chemical and mineralogical evaluation of lateritic soils in humid tropical area (Mfou, Central-Cameroon): Implications for road Construction. *International Journal of Geo-Engineering,* 6:1 DOI 10.1186/s40703-014-0001-0, 21pp.

Kennie, T.J.M., Matthews, M.C. (Eds.). (1985). Remote Sensing in Civil Engineering. Surrey University Press, London.

Kumari, M., Somvanshi, S. (2017). An introduction to remote sensing and its applications (Geoinformatics). Second Edition, S.K. Kataria & Sons, India, 409pp.

Latham, J.P. (Ed.). (1998). Advances in Aggregates and Armourstone Evaluation. Engineering Geology

Special Publication No. 13. Geological Society, London.

Lillesland, T.M., Kiefer, R.W., Chipman, J. (2003). Remote Sensing and Image Interpretation. Wiley, New York.

Martin, F.J., Doyne, H.C. (1927). Laterite and lateritic soils in Sierra Leone. Journal of Agricultural Science, 17: 530-547.

Mayne, P.W. (2001). Geotechnical site characterization using Cone, piezocone, SPTu, and VST, Civil and Environmental Engineering Department, Georgia Institute of Technology

Mayne, P.W. (2007). Cone penetration testing: a synthesis of highway practice. Project 20-5. Transportation Research Board, Washington, D.C. NCHRP synthesis 368.

McNally, G. (1998). Soil and Rock Construction Materials. Spon Press, London.

Meyerhof, G.G. (1956). Penetration tests and bearing capacity of cohesionless soils, Journal of the soil mechanics and foundation division, ASCE, Vol. 82, No. SM1, January, pp. 1-19.

Moss, R.E.S., Seed, R.B., Olsen, R.S. (2006). Normalizing the CPT for overburden stress. *J Geotech Geoenviron Eng* 132(3):378–387. doi:10.1061/(ASCE)1090-0241(2006)132:3(378).

Nigeria Geological Survey (1984). Geological Map of Southwestern Nigeria, Geological Survey Department, Ministry of Mines, Power and Steel, Nigeria.

Nigerian Geological Survey Agency (2006). Geological and Mineral Map of Ondo State, Nigeria.

Ojo, J.S., Olorunfemi, M.O., Akintorinwa, O.J., Bayode, S., Omosuyi, G.O., Akinluyi, F.O. (2015). Subsoil Competence Characterization of the Akure Metropolis, Southwest Nigeria. *Journal of Geography, Environment and Earth Science International*, 2015: 3(1): 1-14. Article no.JGEESI.15851. DOI: 10.9734/JGEESI/2015/ 15851

Olayanju, G.M., Mogaji, K.A., Lim, H.S., Ojo, T.S. (2017). Foundation integrity assessment using integrated geophysical and geotechnical techniques: Case study in crystalline basement complex, southwestern Nigeria. *J Geophys Eng* 14: 675- 690.

Osinowo, O.O., Falufosi, M.O. (2018). 3D Electrical Resistivity Imaging (ERI) for subsurface evaluation in preengineering construction site investigation. *NRIAG Journal of Astronomy and Geophysics*, 1-9pp. https://doi.org/10.1016/j.nrjag.2018.07.001

Oyedele, K.F., Adeoti, L., Oladele, S., Kamil, A. (2014). Investigation of a Proposed Four Story Building Sites Using Geophysical and Laboratory Engineering Testing Methods in Lagos, Nigeria. *International Journal of Scientific Research in Knowledge*, 2(2), pp. 83–91.

Prentice, J.E. (1990). Geology of Construction Materials. Chapman and Hall, London.

Robertson, P.K. (1990). Soil classification using the cone penetration test. Can Geotech J 27:151–158.

Roy, S., Bhalla, S.K. (2017). Role of geotechnical properties of soil on civil engineering structures. Sci Acad Pub 7: 103-109.

Sabins, F.F. (1996). Remote Sensing – Principles and Interpretation. Second Edition, Freeman and Co., San Francisco.

Schmertmann, J.H. (1975). Measurement of insitu shear strength, keynote lecture, Proceedings of the conference *on in-situ measurement of soil properties*, June 1-4, 1975, vol. II, American Society of Civil Engineers.

Smith, M.R., Collis, L. (Eds.). (2001). Aggregates: Sand, Gravel and Crushed Rock Aggregates. Third Edition. *Engineering Geology Special Publication* No. 9. Geological Society, London.

Smith, M.R., (Ed.). (1999). Stone: Building Stone, Rock Fill and Armourstone in Construction. Engineering Geology Special Publication No. 16, Geological Society, London.

Terzaghi, K., Peck, R.B., Mesri, G. (1996). Soil Mechanics in Engineering Practice, 3rd ed., John Wiley Sons Inc.

Tomlinson, M.J. (2001). Foundation Design and Construction. Seventh Edition, Prentice Hall, Harlow, England.

Upadhyay, A.K. (2015). Soil and Foundation Engineering, Second Edition, S.K. Kataria & Sons New Delhi India.349pp.

Ward, W.H., Burland, J.B., Gallois, R.W. (1968). Geotechnical assessment of a site at Mundford, Norfolk, for a large proton accelerator. *Geotechnique*, 18, 399–431

Winkler, E.M. (1973). Stone: Properties, Durability in Man's Environment. Springer-Verlag, New York.

Wright, P.H. (1986). Highway Engineering, Sixth Edition. John Willey and Sons: New York, NY.

Weltman, A.J., Head, J.M. (1983). Site Investigation Manual. Construction Industry Research and Information Association, Special Publication No. 25, London